



**NAVAL
POSTGRADUATE
SCHOOL**

MONTEREY, CALIFORNIA

THESIS

**TRIBOELECTRIC NANOGENERATORS (TENG)
WITH ROTATIONAL MOTION**

by

Joseph A. Kessopha

March 2020

Thesis Advisor:
Second Reader:

Young W. Kwon
Jarema M. Didoszak

Approved for public release. Distribution is unlimited.

THIS PAGE INTENTIONALLY LEFT BLANK

REPORT DOCUMENTATION PAGE			<i>Form Approved OMB No. 0704-0188</i>
Public reporting burden for this collection of information is estimated to average 1 hour per response, including the time for reviewing instruction, searching existing data sources, gathering and maintaining the data needed, and completing and reviewing the collection of information. Send comments regarding this burden estimate or any other aspect of this collection of information, including suggestions for reducing this burden, to Washington headquarters Services, Directorate for Information Operations and Reports, 1215 Jefferson Davis Highway, Suite 1204, Arlington, VA 22202-4302, and to the Office of Management and Budget, Paperwork Reduction Project (0704-0188) Washington, DC 20503.			
1. AGENCY USE ONLY (Leave blank)	2. REPORT DATE March 2020	3. REPORT TYPE AND DATES COVERED Master's thesis	
4. TITLE AND SUBTITLE TRIBOELECTRIC NANOGENERATORS (TENG) WITH ROTATIONAL MOTION			5. FUNDING NUMBERS
6. AUTHOR(S) Joseph A. Kessopha			
7. PERFORMING ORGANIZATION NAME(S) AND ADDRESS(ES) Naval Postgraduate School Monterey, CA 93943-5000			8. PERFORMING ORGANIZATION REPORT NUMBER
9. SPONSORING / MONITORING AGENCY NAME(S) AND ADDRESS(ES) N/A			10. SPONSORING / MONITORING AGENCY REPORT NUMBER
11. SUPPLEMENTARY NOTES The views expressed in this thesis are those of the author and do not reflect the official policy or position of the Department of Defense or the U.S. Government.			
12a. DISTRIBUTION / AVAILABILITY STATEMENT Approved for public release. Distribution is unlimited.			12b. DISTRIBUTION CODE A
13. ABSTRACT (maximum 200 words) Fossil fuels produce most of the world's energy. They have a high energy density, but they release greenhouse gases and are a limited resource. Renewable energy is a relatively new concept that produces low to zero emissions and consists of a variety of methods such as solar, wind, and hydroelectric energy. While the ocean is a very large resource, there is limited research in harvesting energy from it. This research develops and tests a triboelectric nanogenerator (TENG) using rotational motion at the Naval Postgraduate School (NPS). The concept follows previous experiments at NPS with friction between PTFE and copper. The cost and production are reduced by using copper foil tape and PTFE tape and 3D printing the TENG components. The TENG consists of three parts: a top half shell containing half of the copper electrodes, a bottom half containing the other half of the copper electrodes, and an inner rod with PTFE tape. The inner rod is connected to a DC motor and run at various speeds to determine the most effective output voltage and current.			
14. SUBJECT TERMS TENG, wave, triboelectric, generator, voltage, current, power			15. NUMBER OF PAGES 109
			16. PRICE CODE
17. SECURITY CLASSIFICATION OF REPORT Unclassified	18. SECURITY CLASSIFICATION OF THIS PAGE Unclassified	19. SECURITY CLASSIFICATION OF ABSTRACT Unclassified	20. LIMITATION OF ABSTRACT UU

THIS PAGE INTENTIONALLY LEFT BLANK

Approved for public release. Distribution is unlimited.

**TRIBOELECTRIC NANOGENERATORS (TENG) WITH
ROTATIONAL MOTION**

Joseph A. Kessopha
Lieutenant, United States Navy
BS, U.S. Naval Academy, 2013

Submitted in partial fulfillment of the
requirements for the degree of

MASTER OF SCIENCE IN MECHANICAL ENGINEERING

from the

**NAVAL POSTGRADUATE SCHOOL
March 2020**

Approved by: Young W. Kwon
Advisor

Jarema M. Didoszak
Second Reader

Garth V. Hobson
Chair, Department of Mechanical and Aerospace Engineering

THIS PAGE INTENTIONALLY LEFT BLANK

ABSTRACT

Fossil fuels produce most of the world's energy. They have a high energy density, but they release greenhouse gases and are a limited resource. Renewable energy is a relatively new concept that produces low to zero emissions and consists of a variety of methods such as solar, wind, and hydroelectric energy. While the ocean is a very large resource, there is limited research in harvesting energy from it. This research develops and tests a triboelectric nanogenerator (TENG) using rotational motion at the Naval Postgraduate School (NPS). The concept follows previous experiments at NPS with friction between PTFE and copper. The cost and production are reduced by using copper foil tape and PTFE tape and 3D printing the TENG components. The TENG consists of three parts: a top half shell containing half of the copper electrodes, a bottom half containing the other half of the copper electrodes, and an inner rod with PTFE tape. The inner rod is connected to a DC motor and run at various speeds to determine the most effective output voltage and current.

THIS PAGE INTENTIONALLY LEFT BLANK

TABLE OF CONTENTS

I.	INTRODUCTION.....	1
A.	MOTIVATION	1
B.	LITERATURE REVIEW	2
1.	Principle modes of TENG	3
2.	TENG Designs	6
3.	Design Challenges	16
II.	DESIGN DRAFTS	19
A.	DEVELOPMENT	19
B.	MATERIALS	19
C.	DESIGN	21
D.	DESIGN CHALLENGES	33
III.	EXPERIMENTATION PROCESS.....	35
A.	TRANSLATIONAL MOTION TENG (NPS MODEL).....	35
B.	ROTATIONAL TENG PROCESS	38
IV.	RESULTS AND DISCUSSION	49
A.	TESTING TENG INDIVIDUALLY	49
1.	Experimental Results for TENG 1	49
2.	Experimental Results for TENG 2	52
3.	Experimental Results for TENG 3	55
B.	TESTING COMBINING TENG (SERIES AND PARALLEL).....	57
1.	Experimental Results for TENG 4	57
2.	Experimental Results for TENG 5	59
C.	SUMMARY OF ANALYSIS RESULTS	61
1.	Voltage Data	61
2.	Current Data	63
3.	Power Density	64
D.	DISCUSSION	65
V.	CONCLUSION AND FUTURE WORK	67
A.	CONCLUSION	67
B.	RECOMMENDATIONS.....	69
C.	FUTURE RESEARCH.....	70

APPENDIX.....	71
A. TENG 1 DATA.....	71
B. TENG 2 DATA.....	73
C. TENG 3 DATA.....	76
D. TENG 4 DATA.....	79
E. TENG 5 DATA.....	82
 LIST OF REFERENCES.....	 87
 INITIAL DISTRIBUTION LIST	 89

LIST OF FIGURES

Figure 1.	Four fundamental modes of TENG. Source [3].	3
Figure 2.	Structural design of the power-generating shoe insole based on flexible TENGs. Adapted from [4].	4
Figure 3.	Application for single-electrode mode. Source [5].	5
Figure 4.	Design for the wall enclosed ball TENG. Source [5].	7
Figure 5.	Operation for TENG demonstrates vertical separation contact mode. Source [5].	8
Figure 6.	Results for enclosed ball TENG. Source [5].	9
Figure 7.	Demonstration of the practical power for the hybrid nanogenerator. Source [6].	10
Figure 8.	Structural design of hybrid nanogenerator. Adapted from [6].	11
Figure 9.	Diagrams of hybrid nanogenerator at each of four states. Source [6].	12
Figure 10.	Results from testing hybrid nanogenerator. Source [6].	13
Figure 11.	3D and 2D printed parts for NASA Ames design. Adapted from [7].	14
Figure 12.	Demonstration for the friction between the triboelectric layer and the electrodes. Source [7].	15
Figure 13.	Current readings for AP-TENG. Source [7].	16
Figure 14.	SEM image of copper tape.	20
Figure 15.	Results of SEM spectroscopy.	20
Figure 16.	Solidworks image for initial inner rod	22
Figure 17.	Solidworks image for initial design assembly.	22
Figure 18.	3D printed model for first design's inner rod.	23
Figure 19.	3D printed model for first design's outer shell.	23
Figure 20.	Solidworks design for with new diameter for the inner rod.	24
Figure 21.	Solidworks assembly for the second design.	25

Figure 22.	3D printed model of inner rod for second design.	25
Figure 23.	3D printed model for outer shell for second design.....	26
Figure 24.	Solidworks assembly for third design.....	27
Figure 25.	3D printed assembly of third design with electrodes.....	28
Figure 26.	Solidworks design of the final design for the inner rod.....	29
Figure 27.	Solidworks assembly of the final TENG design.....	30
Figure 28.	3D printed assembly of final TENG design.....	30
Figure 29.	Design for TENG electrode tracks with 1.27 cm (½ in) fingers. (Left) Initial design (right) improved design.	31
Figure 30.	Design for TENG electrode tracks at (left) 0.635 cm (¼ in) and (right) 3 mm fingers.	32
Figure 31.	First NPS TENG model. Source [9].	35
Figure 32.	Final assembly of initial NPS TENG model. Source [9].	36
Figure 33.	Schematic of second version of NPS TENG model. Source [10].....	37
Figure 34.	Final assembly of second NPS TENG. Source [10].	38
Figure 35.	DC motor drives inner rod for TENG.....	39
Figure 36.	Digital tachometer.....	40
Figure 37.	Teng assembly with wires attached to electrodes. and reflective tape for tachometer.	41
Figure 38.	Top view of TENG with electrodes and lead.....	42
Figure 39.	Load attached to TENG to gather current readings.	42
Figure 40.	Tektronix T CPA300 amplifier connects to the TENG and oscilloscope.....	43
Figure 41.	Amplifier attached to Tektronix MSO 4034.....	44
Figure 42.	Keithley 617 Electrometer.	45
Figure 43.	Lead connections from the TENG to the electrometer.	45

Figure 44.	Two TENGs connected in series.....	46
Figure 45.	Connecting TENG in parallel.	47
Figure 46.	Average voltage data for TENG 1.	50
Figure 47.	Average current for TENG 1.	51
Figure 48.	Power density for TENG 1.	52
Figure 49.	Average voltage data for TENG 2.	53
Figure 50.	Average current for TENG 2.	54
Figure 51.	Power density for TENG 2.	54
Figure 52.	Average voltage for TENG 3.....	55
Figure 53.	Average current for TENG 3.	56
Figure 54.	Power density for TENG 3.	57
Figure 55.	Average voltage for TENG 4.....	58
Figure 56.	Current for TENG 4.....	58
Figure 57.	Power density for TENG 4.	59
Figure 58.	Average voltage for TENG 5.....	60
Figure 59.	Average current for TENG 5.	60
Figure 60.	Power density for TENG 5.	61
Figure 61.	Voltage summary plot.....	62
Figure 62.	Current summary plot.	63
Figure 63.	Power summary.	64
Figure 64.	Power density summary.....	65
Figure 65.	TENG 1 current readings for each speed.....	71
Figure 66.	Voltage for TENG 1 at 360 rpm.	72
Figure 67.	Voltage for TENG 1 at 240 rpm.	72
Figure 68.	Voltage for TENG 1 at 120 rpm.	73

Figure 69.	Voltage for TENG 1 at 60 rpm.	73
Figure 70.	TENG 2 current readings for each speed.	74
Figure 71.	Voltage for TENG 2 at 360 rpm.	74
Figure 72.	Voltage for TENG 2 at 240 rpm.	75
Figure 73.	Voltage for TENG 2 at 120 rpm.	75
Figure 74.	Voltage for TENG 2 at 60 rpm.	76
Figure 75.	TENG 2 current readings for each speed.	77
Figure 76.	Voltage for TENG 3 at 360 rpm.	77
Figure 77.	Voltage for TENG 3 at 240 rpm.	78
Figure 78.	Voltage for TENG 3 at 120 rpm.	78
Figure 79.	Voltage for TENG 3 at 60 rpm.	79
Figure 80.	TENG 4 current reading for each speed.	80
Figure 81.	Voltage for TENG 4 at 360 rpm.	80
Figure 82.	Voltage for TENG 4 at 240 rpm.	81
Figure 83.	Voltage for TENG 4 at 120 rpm.	81
Figure 84.	Voltage for TENG 4 at 60 rpm.	82
Figure 85.	TENG 4 current reading for each speed.	82
Figure 86.	Voltage for TENG 5 at 360 rpm.	83
Figure 87.	Voltage for TENG 5 at 240 rpm.	84
Figure 88.	Voltage for TENG 5 at 120 rpm.	84
Figure 89.	Voltage for TENG 5 at 60 rpm.	85

LIST OF TABLES

Table 1.	Surface area for electrode and spacing between fingers for one half of the TENG.....	32
Table 2.	Surface area of the combined halves of the TENG.....	33
Table 3.	Voltage data (V) summary table.....	62
Table 4.	Current (nA) summary table.....	63
Table 5.	Power (nW) summary table.....	64
Table 6.	Power density ($\mu\text{W}/\text{m}^2$) summary table.....	65

THIS PAGE INTENTIONALLY LEFT BLANK

LIST OF ACRONYMS AND ABBREVIATIONS

ABS	acrylonitrile butadiene styrene
AC	alternating current
AP-TENG	all-printed triboelectric nanogenerator
DC	direct current
EMG	electromagnetic generator
FEP	fluorinated ethylene propylene
LED	light emitting diode
NOAA	National Oceanic and Atmospheric Administration
NPS	Naval Postgraduate School
OC	oscillating column
PENG	piezoelectric nanogenerator
PETG	polyethylene terephthalate
PLA	polylactic acid
PMMA	polymethyl methacrylate
PTFE	polytetrafluorethylene
RMS	root mean square
RPM	rotations per minute
SEM	scanning electron microscope
S-TENG	spiral-interdigitated-electrode triboelectric nanogenerator
TEG	thermoelectric generator
TENG	triboelectric nanogenerator
TPU	thermoplastic polyurethane
W-EMG	wrap-around electromagnetic generator

THIS PAGE INTENTIONALLY LEFT BLANK

ACKNOWLEDGMENTS

First and foremost, I would like to thank Dr. Kwon for his guidance and patience while I attended the Naval Postgraduate School. I would also like to thank Professor Didoszak for his assistance while working on my thesis. I am indebted to the RoboDojo and their invaluable expertise in assisting in printing my parts. I would like to give a special thanks to Warren Rogers and Frankie Blevins for their knowledge in test equipment. I would like to personally thank Sarah Reilly and Katherine Mann for their invaluable knowledge and previous TENG research.

I would like to give a special shoutout to Richard McClain, because without him, I would probably still be trying to figure out how to use Solidworks. Finally, I would like to thank my family and the friends I have made while in Monterey for helping me stay sane.

THIS PAGE INTENTIONALLY LEFT BLANK

I. INTRODUCTION

A. MOTIVATION

Over the last few decades, the demand to power electronics increases as technology advanced. Fossil fuels and natural gases continue to remain as the primary power production in the world. These types of fuel have a very high energy density and are a reliable source for power. The caveat is that these fuels are a limited resource and release greenhouse gases that harmful to the environment, raising concerns such as climate change. The demand for alternative energy has become more imperative as a result.

Solar, wind, and water turbine energy are a few alternative green energy methods that developed over the last few decades to combat the concern for global warming. Throughout the last decade there has been a large increase in solar and wind farms to harvest energy required for our daily needs. In 2018, the average American citizen used approximately 309 million British Thermal Units (BTU), approx. 90,500 kWh, while the average for the rest of the world was 77 million BTU [1]. The demand for energy will continue to increase, therefore it is imperative to continue to use alternative energy to combat our impending concerns.

The earth is nearly 71% water; however, the only commercial method to harvest energy through water is using hydroelectric dams, which is limited to regions with rivers. Solar and wind farms do not produce much energy for land they require for building. The environment also greatly affects the energy output for these types of generators. Obviously, they cannot produce energy at night or when there is no wind, respectively. If we can harvest energy from the ocean, we can increase our supply for electricity to meet our demand for global energy. This will be more feasible to power coastal cities, since human population thrive mainly near the coast. Most importantly, it is a continuous source of energy, unlike other alternative energy methods.

Energy can be harvested from the ocean by utilizing the constant wave motion. In theory, the ocean is a source that can produce green energy for the entire world. The

problem in this technology is in its early stages of development and unlikely to be mass produced soon.

The pros for harvesting energy from ocean waves include high energy density, huge source, and waves will always be a continuous source. As with anything in the ocean, there are several challenges. One major challenge is maintenance. It could cost more resources to maintain generators in the ocean or to manufacture a product capable of withstanding the harsh ocean waves. Another is developing a generator that is corrosion resistant. Due to their high-power output from low frequencies, triboelectric nanogenerators (TENGs) are the preferred method in this research to harvest the ocean energy. Triboelectric means contact electrification, mainly through friction. Nanogenerators indicate converting mechanical motion with a small-scale change into electricity.

B. LITERATURE REVIEW

The triboelectricity is generating electricity through friction. This effect happens when two dissimilar materials contact each other. Once in contact, electrons flow from one material to the other and cause a potential drop which is voltage. This effect is seen through various magic tricks such as rubbing a balloon on a person's hair then sticking it to a wall. Another demonstration would be to wear wool socks on a carpet to generate charge to shock a younger or older sibling. This seemingly whimsical effect can have much more practical applications and lead to a future in advancement in blue energy. Various TENG designs utilize different materials and wave motion to reproduce this effect to generate electricity.

Research teams from the National Aeronautics and Space Administration (NASA) and various universities from South Korea, China, and United States designed and experimented with various renditions of the TENG for a multitude of applications. Applications include personal TENG's to charge personal electronics, to harvesting ocean waves, and using TENG's to power electronics in space.

Research for the TENG is extensive and varies from optimizing the types of materials to optimal designs for harvesting wave energy. The common denominator in the

various research is copper is the ideal electrode and friction between copper and a piezoelectric material such as polytetrafluorethylene (PTFE) generate optimal electricity. Frequency at each contact point is the factor that determines the voltage output for the TENG. As the two different materials come into contact, a chemical process called adhesion occurs and charge transfers from one material to the other to equalize the chemical potential, thus producing voltage [2].

1. Principle modes of TENG

Based off the principle of transferring charge through friction, there are four principle modes for a TENG, which are vertical contact-separation, contact sliding, single electrode, and freestanding triboelectric-layer mode [2].

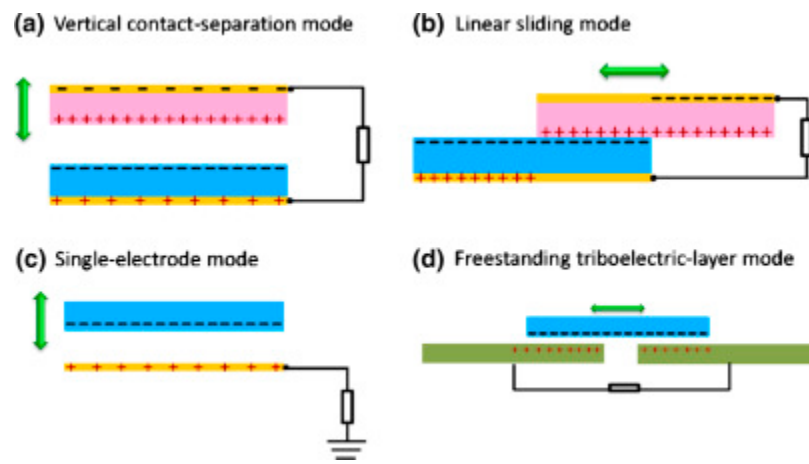
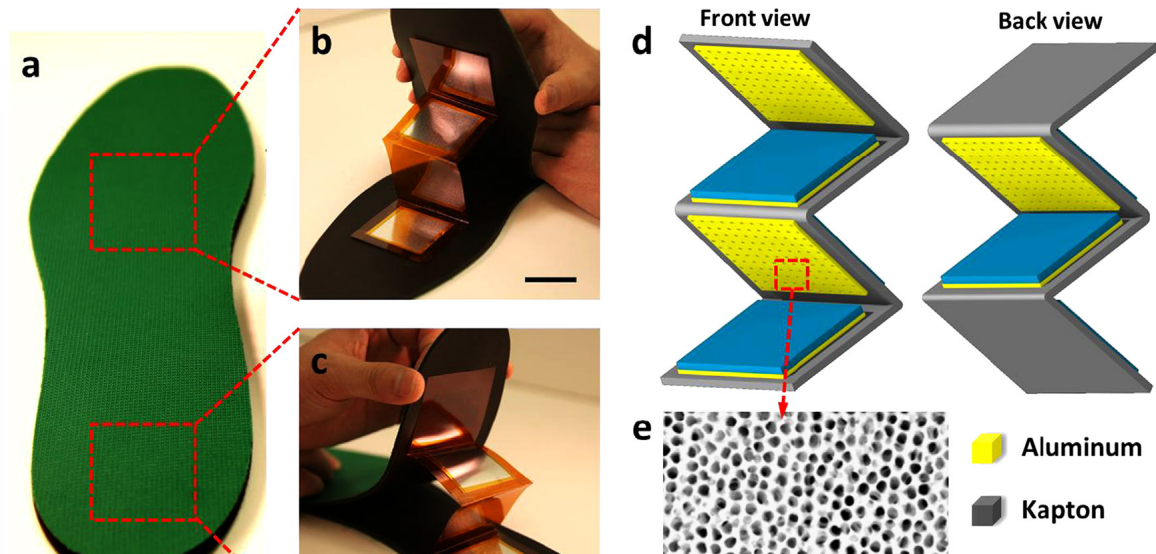


Figure 1. Four fundamental modes of TENG. Source [3].

a. Vertical contact separation

Vertical contact separation is the simplest TENG design with having two dissimilar dielectric film in contact and having an electrode placed on the top and bottom [3]. The two are placed in contact, then separated by a small gap through an external force. This creates potential drop which transfers the free electrons from one electrode to the other until the two materials come into contact again. This mode of TENG is limited to linear motion to support the movement which limits design concepts. Figure 2 shows an

experiment conducted by students at Georgia Institute of Technology and Beijing Institute of Nanoenergy and Nanosystems that demonstrates using the vertical separation mode for a TENG by placing it in an insole to harvest energy from walking.



(a) TENG that utilizes walking to generate electricity. (b) Inner structure of TENG in the insole. (c) Other side of the insole with TENG. (d) Inner make up of TENG structure with materials. (e) Zoom in of the aluminum electrodes with Kapton infused.

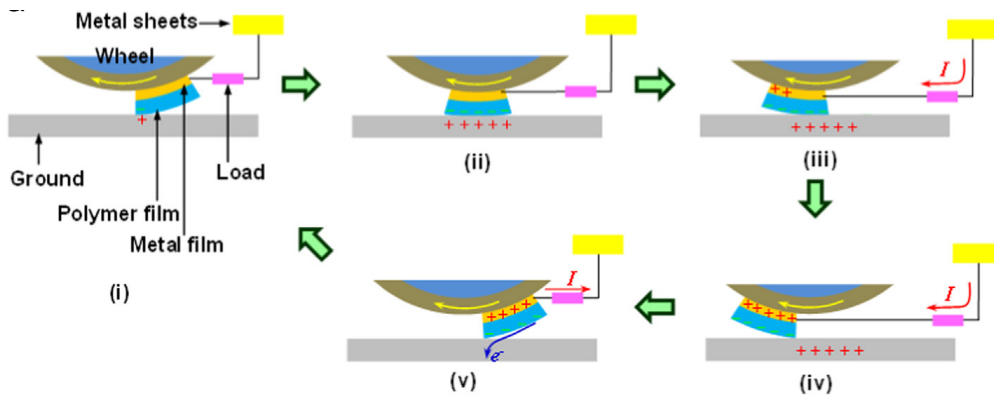
Figure 2. Structural design of the power-generating shoe insole based on flexible TENGs. Adapted from [4].

b. Contact sliding

Contact sliding is set up the same as vertical contact-separation. When the two dielectric materials slide parallel to each other, they generate a triboelectric charge on the two surfaces. This induces a lateral polarization in the sliding direction resulting in transferring electrons to the top and bottom electrodes, which balances the area created by triboelectric charges [3]. Contact sliding creates an alternating current (AC) output and can have various methods such as disk rotation, cylindrical rotation, and planar motion. The NPS design emulates this mode.

c. Single-electrode

Single-electrode mode is where an object that is part of the TENG cannot be connected to the load because it is continually in motion. This TENG design harvests energy with a single electrode that is grounded at the bottom. Motion above the electrode will transfer electrons between the bottom electrode and ground, therefore allowing a potential change [3]. This effect is notable in the previous two modes as well. Figure 3 shows an experiment conducted from students from University of Wisconsin and Zhengzhou university that demonstrate the application of a single electrode mode for a TENG.



This TENG application utilizes single-electrode mode to generate electricity from the friction between a car tire and the TENG.

Figure 3. Application for single-electrode mode. Source [5].

d. Freestanding triboelectric-layer

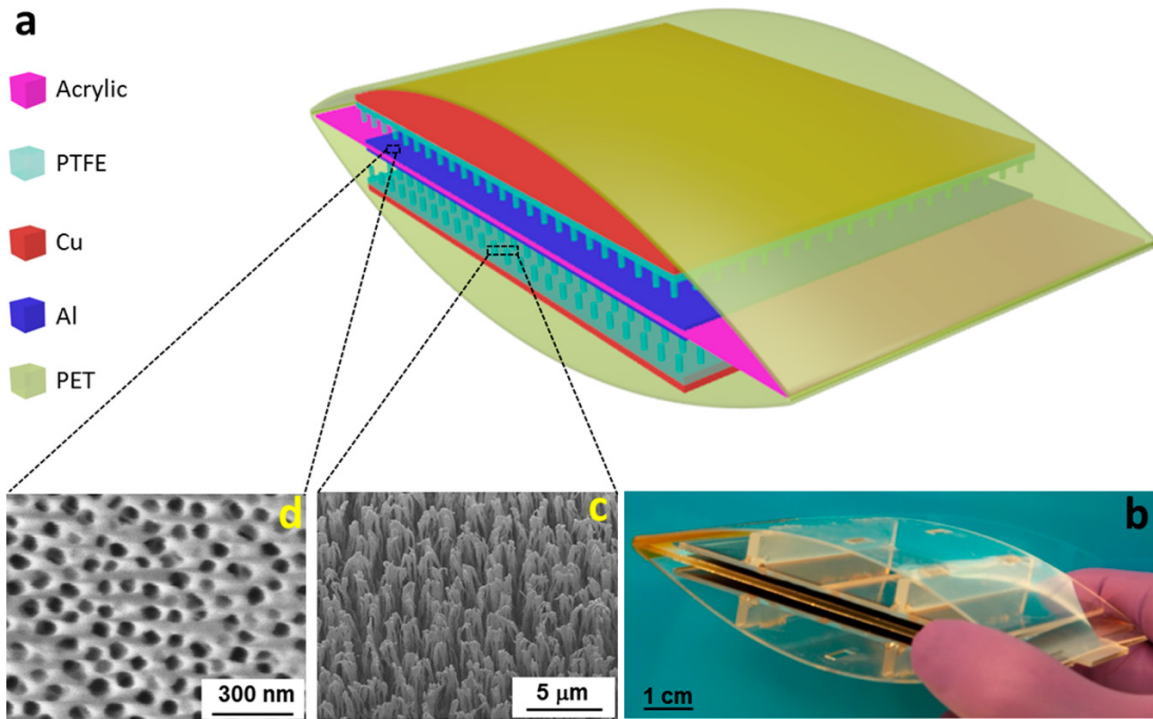
The freestanding triboelectric-layer mode is harvesting energy from freely moving objects without connection to a source. This mode considers that all surfaces in objects have a charge. Charge will generate by placing two parallel symmetric electrodes underneath a dielectric layer and sizing the gap to the moving object. This will cause electrons to flow between the two electrodes [3].

2. TENG Designs

TENGs optimize power through slow, multidirectional motion, into electrical power, while being lightweight, and cheap to produce [5]. Since the nature of ocean waves is random and varying in frequency, TENGs are ideal for harvesting such energy. One issue is it can only produce enough electricity to power small scale electronics, such as LED lightbulbs and sensors. A network of TENG's would solve such an issue to meet more demanding requirements. It is also important to consider the energy density of one TENG to observe how the network of TENG multiplies the power output.

a. Enclosed ball TENG

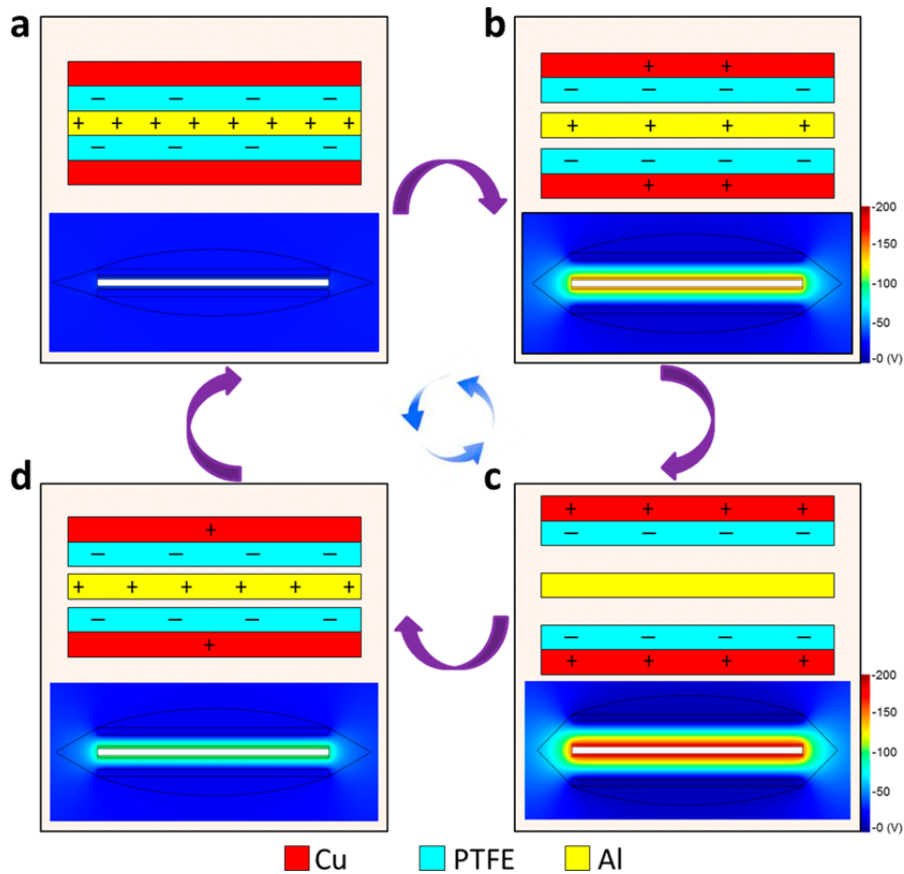
Simple TENG designs rely on friction in two directions to generate power. Since ocean waves are unpredictable, it is difficult to design a TENG that can account for the unpredictable movement. This design utilizes an enclosure with four identical TENGs are the wall for the structure. As shown in Figure 4, the outer shell consists of polyethylene terephthalate (PET) to protect the inner components. Compressing the PET shell will connect the electrodes and releasing will separate the electrodes, generating the triboelectric effect. The acrylic acts as a barrier between the top and bottom half separating the two sets of electrodes. As shown, there is a thin film of PTFE that separates the copper from the aluminum.



(a) Composition of the TENG wall. (b) Picture of actual TENG, demonstrating size. (c) SEM image of PTFE. (d) SEM image of aluminum pores.

Figure 4. Design for the wall enclosed ball TENG. Source [5].

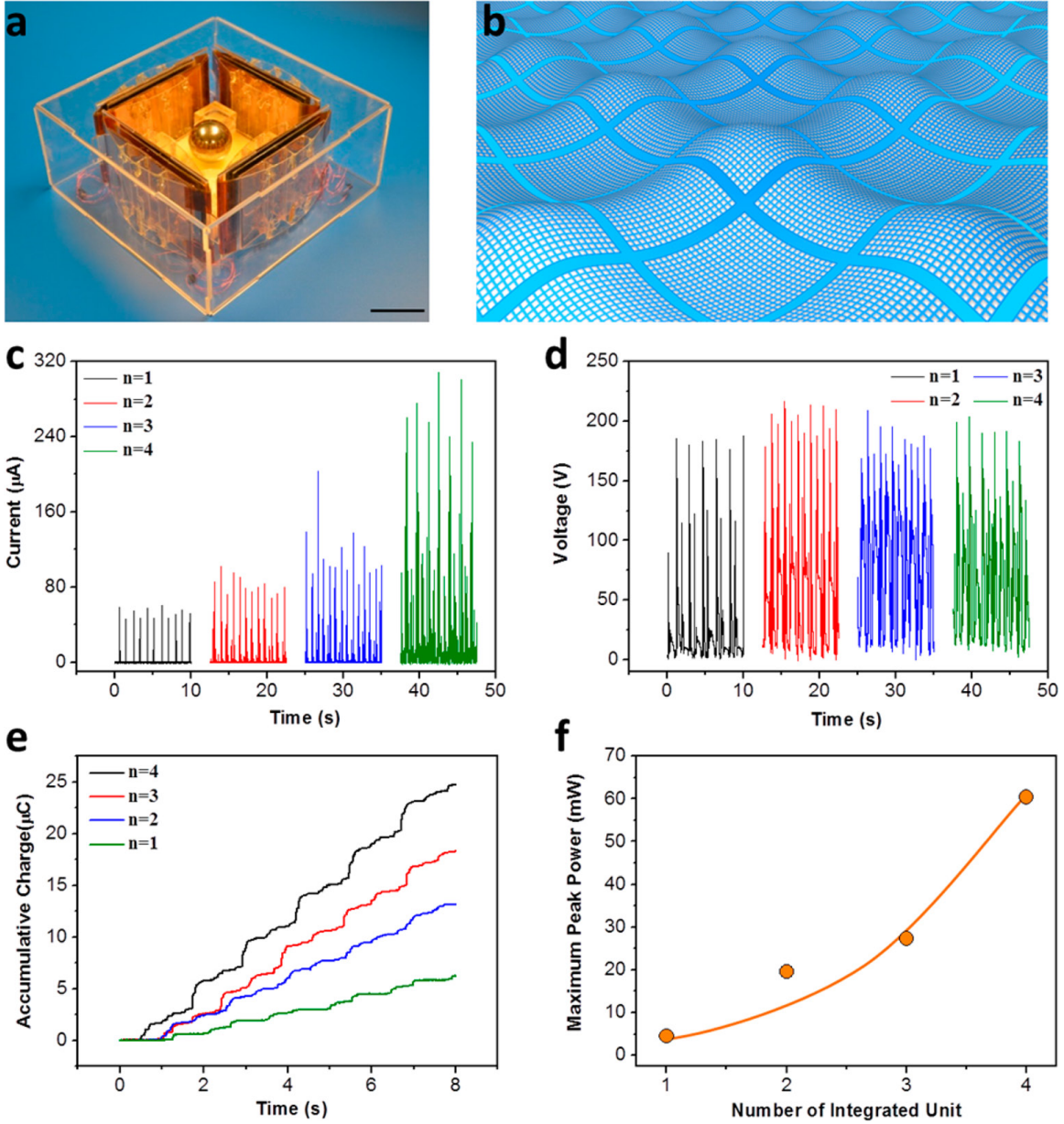
This experiment demonstrated the effectiveness of connecting 4 TENG units in series. Figure 5 shows what the build for each individual TENG. The ball acts with the ocean waves and uses gravity to push into the TENG walls. This activates the reaction between the electrode and triboelectric layer, generating electricity.



(a) Triboelectric layer and electrodes are in contact with each other. (b) Initial separation for the two layers. (c) Maximum separation between electrode and triboelectric layer. (d) Electrode and triboelectric layers returning to contact.

Figure 5. Operation for TENG demonstrates vertical separation contact mode. Source [5].

Figure 6 shows the results for the TENG performance. The power output for an individual TENG is very low but increases exponentially when adding more in series. The TENG in series was enough to power a series of light emitting diodes (LED) lights. Individually the TENG is not practical, but a network of TENG can produce large power.



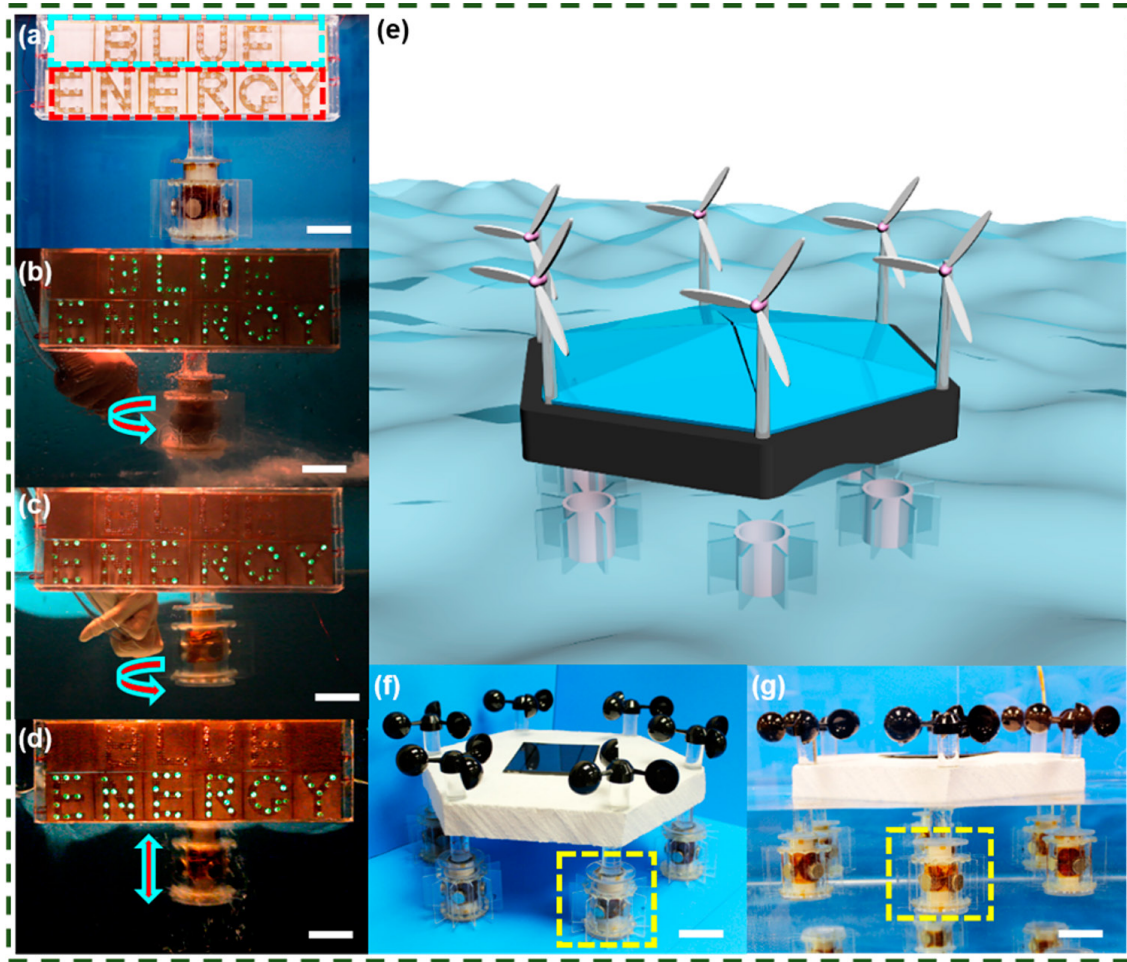
(a) Final build of the TENG with 4 walls. The wave motions move the ball to depress the TENG. (b) Visual for TENG network. (c-f) Readings for current, voltage, charge, and power for the TENG. N represents the number of TENG attached in series.

Figure 6. Results for enclosed ball TENG. Source [5].

b. Electromagnetic hybrid nanogenerator

A coalition of researchers from various universities developed a hybrid generator that utilized triboelectric and electromagnetic generation to harvest ocean energy. The hybrid design consisted of a spiral-interdigitated-electrode triboelectric nanogenerator (S-

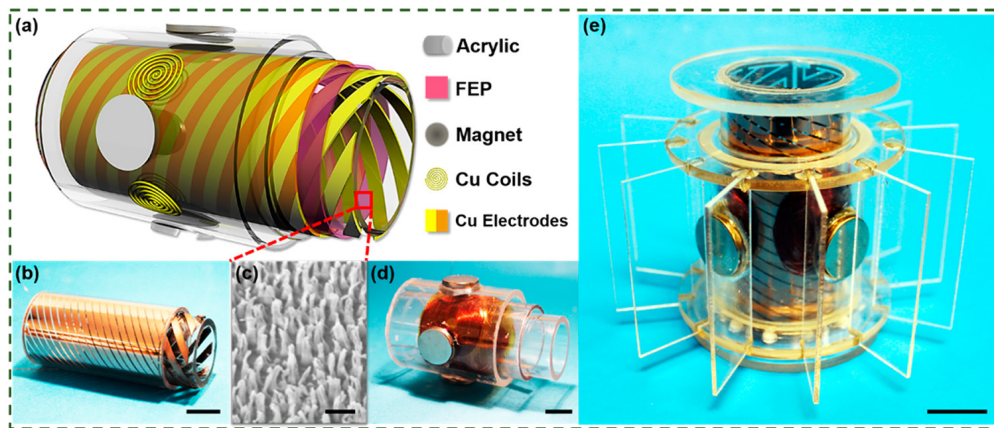
TENG) and a wrap-around electromagnetic generator (W-EMG). Both the W-EMG and S-TENG are designed to generate electricity from both rotational and linear motion. Figure 7 shows the concept art for the hybrid generator along with powering an LED sign from the various ranges of motion.



(a) The W-EMG powers the LED's that spell the word "BLUE" while the S-TENG power the LED's that spell the word "ENERGY." (b) Demonstration of rotation above water. (c) Demonstration of rotation below water. (d) vertical motion above water. (e) Illustration of hybrid network of nanogenerators. (f) Oblique angle view. (g) Lateral view. The white bar is a scaled to 10cm.

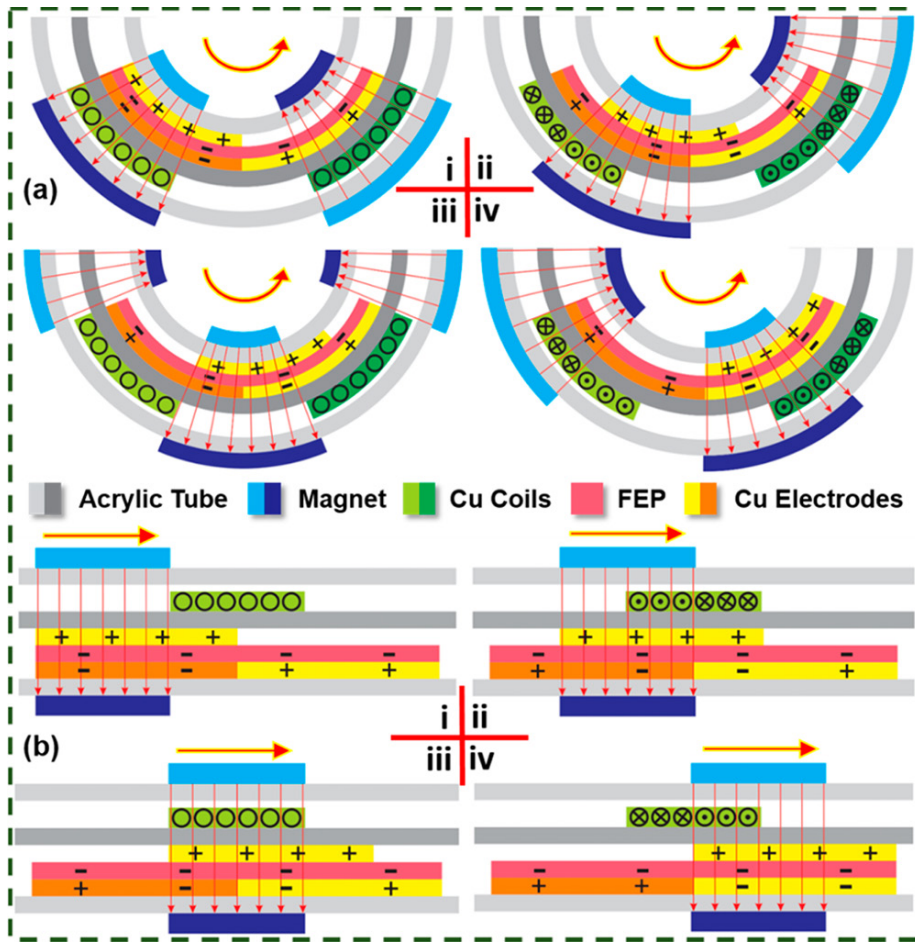
Figure 7. Demonstration of the practical power for the hybrid nanogenerator. Source [6].

The S-TENG utilizes friction between spiral-interdigitated electrodes along with fluorinated ethylene propylene (FEP) strips, which act to harvest both rotational and translational motion. The magnet in the W-EMG assists the S-TENG in moving, therefore generating more power. Figure 9 demonstrates how the copper electrodes in the S-TENG move along with the W-EMG. Rotational motion was tested with an electric motor that ranged from 10–300 rpm, while a linear reciprocating motor simulated fluctuation that ranged from 1 to 5 Hz [6].



(a) Schematic of all components of the hybrid TENG. (b) S-TENG components. (c) SEM image of the FEP nanowires. (d) W-EMG components. (e) Complete construction of hybrid nanogenerator.

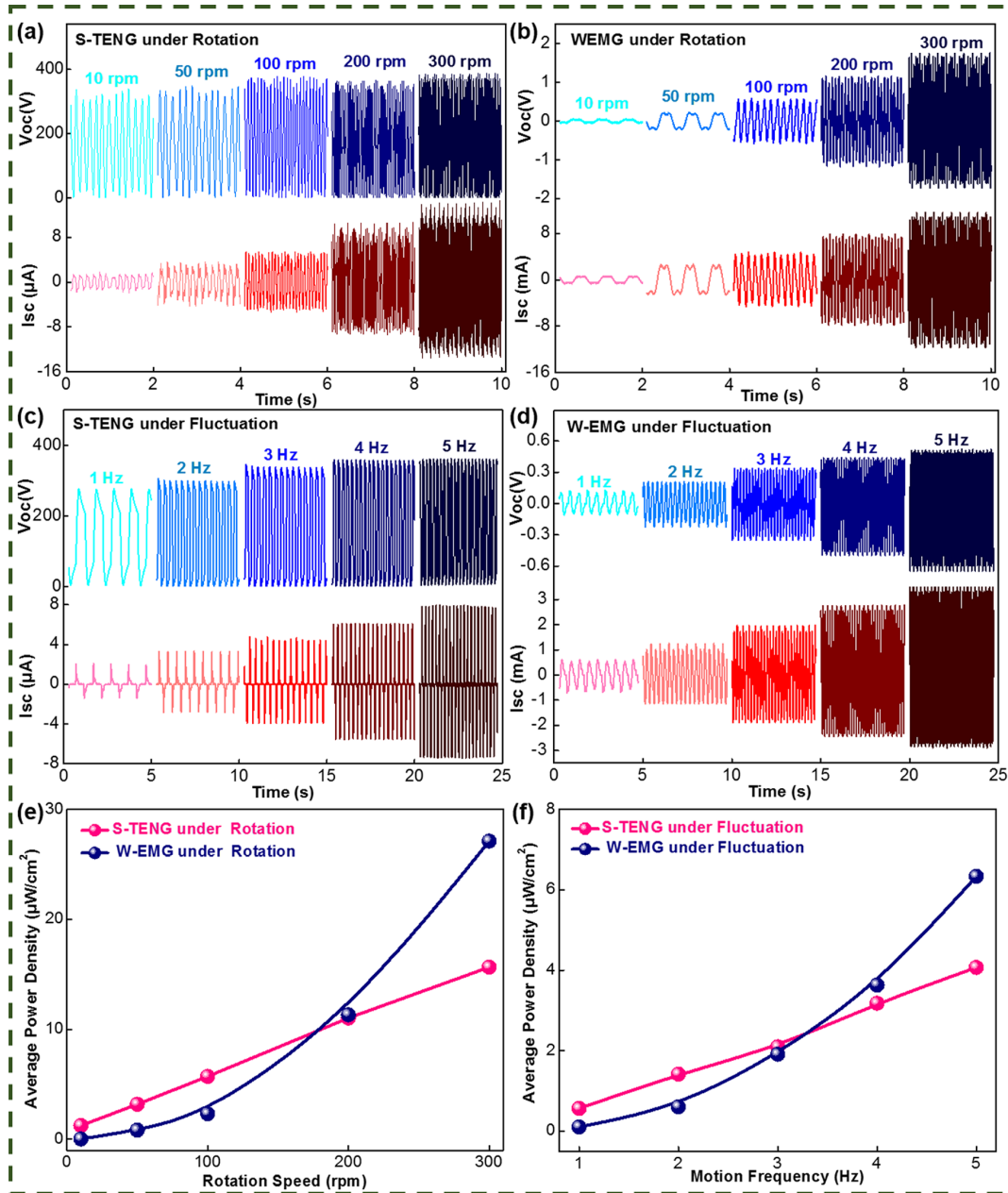
Figure 8. Structural design of hybrid nanogenerator. Adapted from [6].



(a) Rotational mode. (b) Fluctuation mode.

Figure 9. Diagrams of hybrid nanogenerator at each of four states. Source [6].

As shown in Figure 10, the S-TENG does not produce as high a current as the W-EMG. The S-TENG produces high voltage at all frequencies, making it a viable option for generating energy. In the practical demonstration the nanogenerator produced enough electricity to power the LED sign.



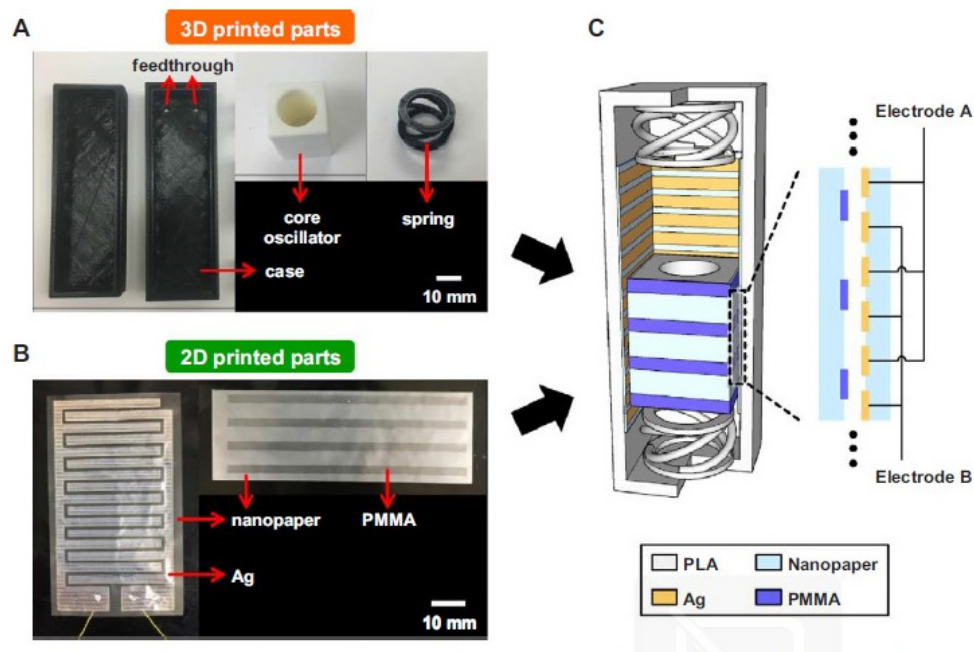
(a-f) Various specifications of performance from the each generator and comparison of fluctuation vs rotation.

Figure 10. Results from testing hybrid nanogenerator. Source [6].

c. All-printed Triboelectric Nanogenerator (AP-TENG)

The NASA Ames research center and researchers at Seoul National University in the Republic of Korea tested a design for an AP-TENG. All components for this TENG are fabricated with a 3D printer using polylactic acid (PLA) and the electrodes cut with a 2D

printer. The design utilized friction between polymethyl methacrylate (PMMA) and silver electrodes. The advantages of all 3D printed parts are its cheap, easy to reproduce, environmentally friendly, and highly customizable [7]. The challenge with printing the components is to ensure the parts are precise sizes. If the parts are printed too small, it will reduce the contact friction between the electrode and triboelectric layer. If the parts are printed too large, it will increase the contact friction between the electrode and triboelectric layer and potentially prevent a full range of motion for the TENG.



(a) 3D printed parts. (b) 2D inkjet-printed parts for electrodes. (c) A schematic of AP-TENG assembly

Figure 11. 3D and 2D printed parts for NASA Ames design. Adapted from [7].

The width of the grating lines for each of the interdigitated fingers are 3 mm and the spacing between opposing fingers is 1.5 mm. The widths of the grating lines for the PMMA layer is 6 mm to account for overlapping the two different layers.

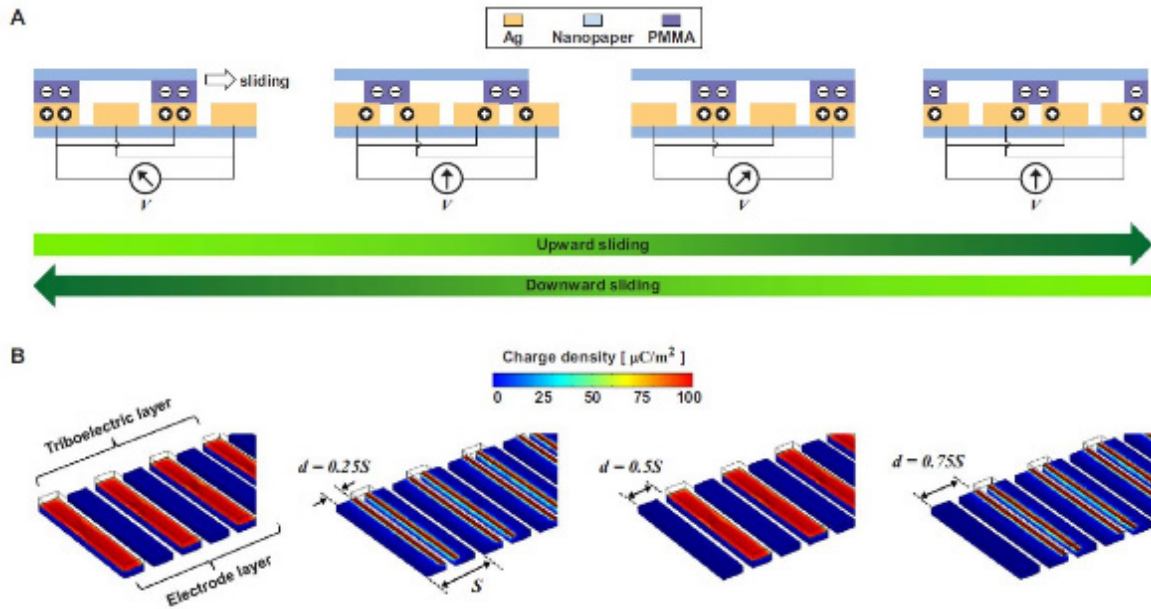
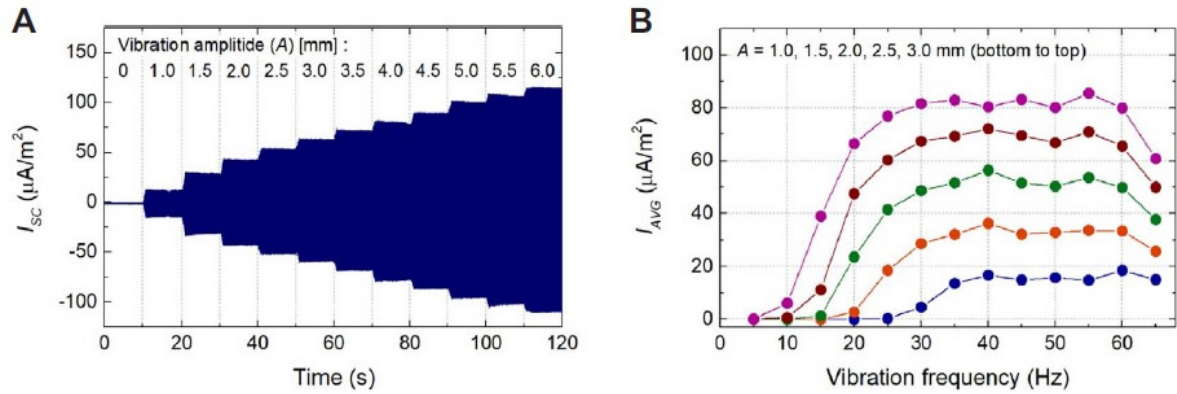


Figure 12. Demonstration for the friction between the triboelectric layer and the electrodes. Source [7].

The triboelectric layer, made of PMMA, is negatively charged which attracts the positive charges in the electrode. When the triboelectric layer is completely overlapped with one electrode, it accumulates a positive counter charge with the corresponding electrodes. As the triboelectric layer overlaps the electrode, it transfers a positive counter charge between the two electrodes, increasing electrical energy [7]. Figure 13 shows how the vibration frequency affects the amplitude for the current. It is important to note the current is in the microamps. The higher the vibration frequency, the higher the current. The open circuit voltage has a load of 200 teraohms ($\text{T}\Omega$) and the short circuit a load of 2 ohms (Ω) [7].



(a) Graph out output current, I_{SC} , vs time. (b) Plot of output current, I_{AVG} , at various frequencies.

Figure 13. Current readings for AP-TENG. Source [7].

3. Design Challenges

As with anything that operates in the ocean, there are a multitude of challenges for this task. Harvesting energy from ocean waves proves a difficult process because most generators, such as EMGs, collect energy from high frequency, high power rotation [3]. Since ocean waves are low frequency, the challenge arises to have a generator that can provide a high-power output using low frequency. TENGs are ideal for this task because they produce such a huge voltage drop from the friction [3, 5–7]. Unfortunately, there are several issues that also arise in producing a TENG.

The common problems with TENG designs equate to three major challenges: durability, power, and a practical design for ocean application [3, 6–10]. The triboelectric effect is transferring charges from one material to another dissimilar material. This occurs through friction, which most materials will fatigue under constant frictional force. The longer materials continue to rub against each other, the more likely it is to fail. Reducing friction or limiting the motion for the TENG will mitigate this issue.

TENGs produce high power in low frequencies [3]. TENGs produce a very high voltage while operating, however, the current is very minimal. Most TENGs produce current in the nanoamps and have a maximum in the microamps [6-10]. This severely reduces the power output for the nanogenerators. Some experiments connected TENGs to

observe the increased power output, which mitigated the power deficiency [6-8]. Had there been a large farm of TENGs, the power output would multiply to a useable amount.

Since the concept of TENGs is a new concept, the application is in development and experiments are more of proof of concept. There are several design challenges in manufacturing a TENG that goes into the water. It is easy to develop and waterproof a TENG because the parts are internal, however if it is completely sealed off, it becomes impossible to connect one TENG to another.

THIS PAGE INTENTIONALLY LEFT BLANK

II. DESIGN DRAFTS

A. DEVELOPMENT

The general idea for the TENG is to generate electricity through friction between two piezoelectric materials. For this test, friction between copper and PTFE tape generates electricity. Previous designs utilize friction through linear motion. It was determined that the frequency between contact points is the greatest affecting factor. The design used for this experiment utilizes rotational motion to determine its effectiveness. Rotational motion will allow frequency adjustments through varying gear ratios, which will allow more power output for the TENG.

The Naval Postgraduate School (NPS) in Monterey, California designed a TENG that emulated the NASA Ames Research Center's Center for Nanotechnology in Moffett Field, California [6, 9, 10]. This design relied on 2D and 3D printed materials for fabrication. The 3D printer fabricated the cradle, while the 2D printer cut the copper electrodes into shape.

B. MATERIALS

This TENG design utilized the same materials as the previous NPS design. Copper foil tape replaced the 2D cut copper sheet for the anode to facilitate application to the TENG's curved design. Copper tape is available for purchase through commercial retailers, making it easily accessible. A sample of the tape was placed in the scanning electron microscope (SEM) to determine its purity. The results determined the tape is pure copper. As shown in Figure 14 and Figure 15, the copper tape is pure copper, which makes the tape ideal for use in the TENG.

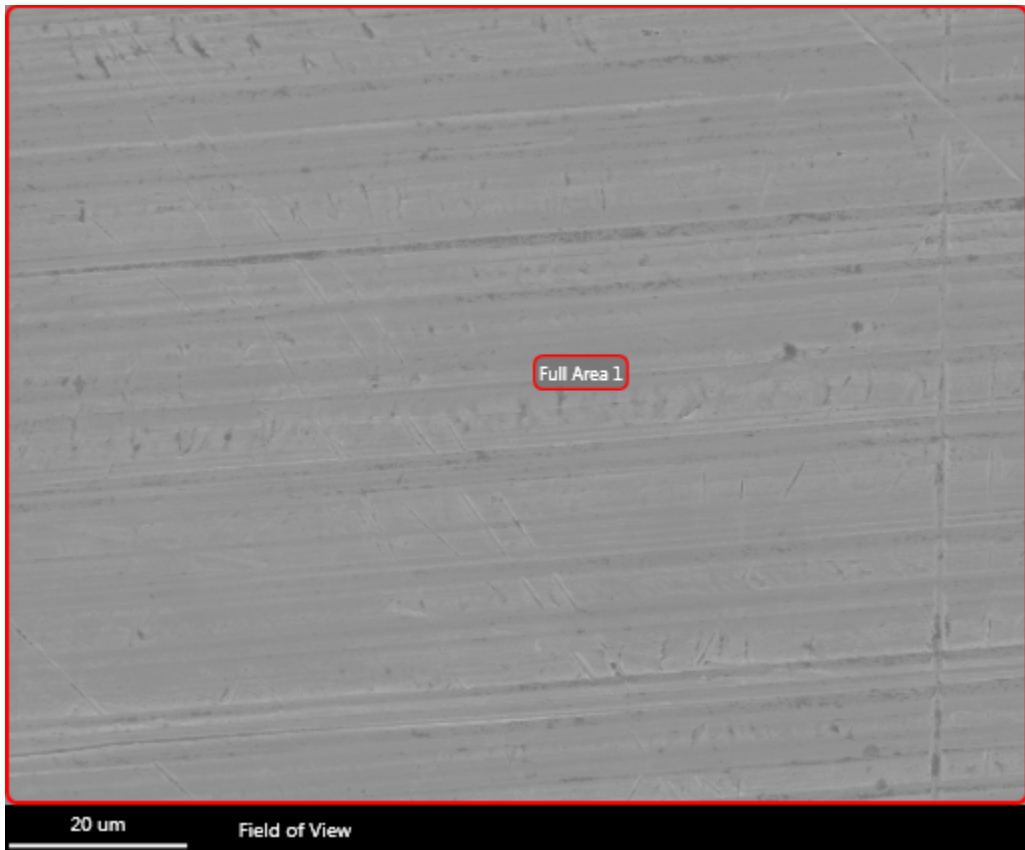


Figure 14. SEM image of copper tape.

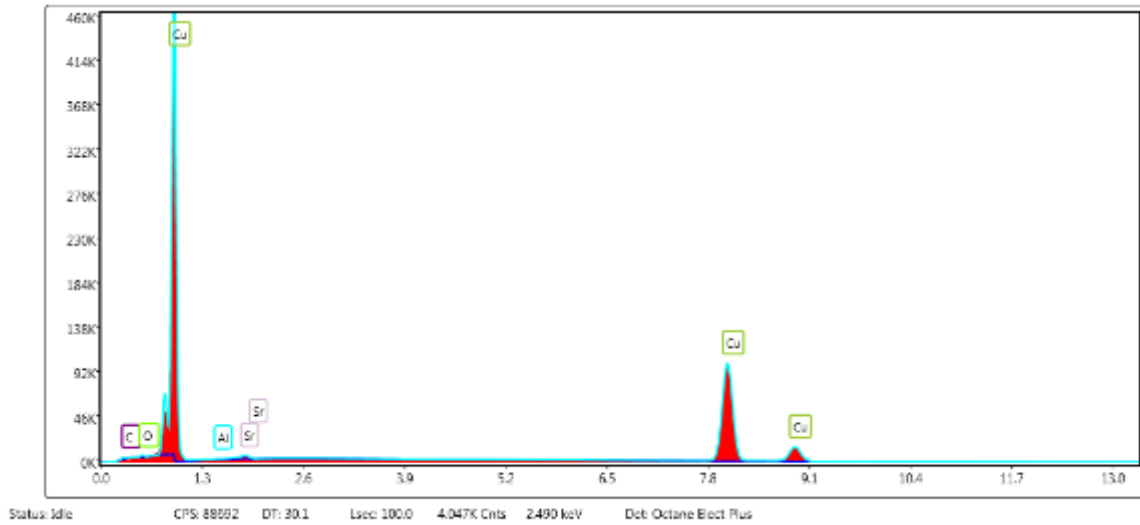


Figure 15. Results of SEM spectroscopy.

The different filament options to print the TENG were polylactic acid (PLA), acrylonitrile butadiene styrene (ABS), polyethylene terephthalate (PETG), and thermoplastic polyurethane (TPU). The advantage for PLA is the durability and is the standard filament for most 3D printers because it is a material that is easy to print. The challenge with PLA is that it is not a weather resistant material and highly water soluble. ABS is a very durable material that is used in most protective equipment. The issue is the material is very difficult to print and requires settings that are not available in most affordable 3D printers. PETG is a water-resistant material that is durable and has the same characteristics as PLA. The issue with PETG is it is not as common and readily available as PLA. TPU is a flexible material that would mitigate some issues with the TENG and sizing, however, it is a very difficult material to print and is very water soluble. The TENG structure was printed on a 3D printer using PLA because it is the easiest of the materials to work with and is durable enough to handle the experiments.

C. DESIGN

The goal for the design for the TENG is to have rod spin freely within a shell that would produce electricity. From the previous NPS design, the TENGs had moving electrodes on a stationary track with PTFE. It would not be ideal to connect wires to rotating parts for the new design because it could cause damages. For this reason, the spinning rod contains the PTFE tracks while the outer shell, which remains stationary, contains the electrodes.

The program used to design the TENG components is Solidworks 2018. Each part was converted to a SLT file. The files were sent to the applications Ultimaker Cura ver 4.4 to format for 3D printing. The dimensions for the components in Solidworks 2018 are in cm. The 3D printer used to print the TENG designs is a Creality Ender 5.

The first TENG design did not consider matching the spacing between the electrode fingers with the PTFE tape. The spacing for the PTFE tape was half an inch with 8 strips along the inner rod. According to the NASA design, the spacing between the fingers on one side of the electrode must match the spacing between the PTFE tape. This will allow one side of electrodes to contact the tape while the other electrode does not. The original

design had a diameter of 6.48 cm. This was determined through the size of the circumference, which was the size of the tape 1.27 cm 0.5 (in) times 16 (number of strips of tape multiplied by 2).

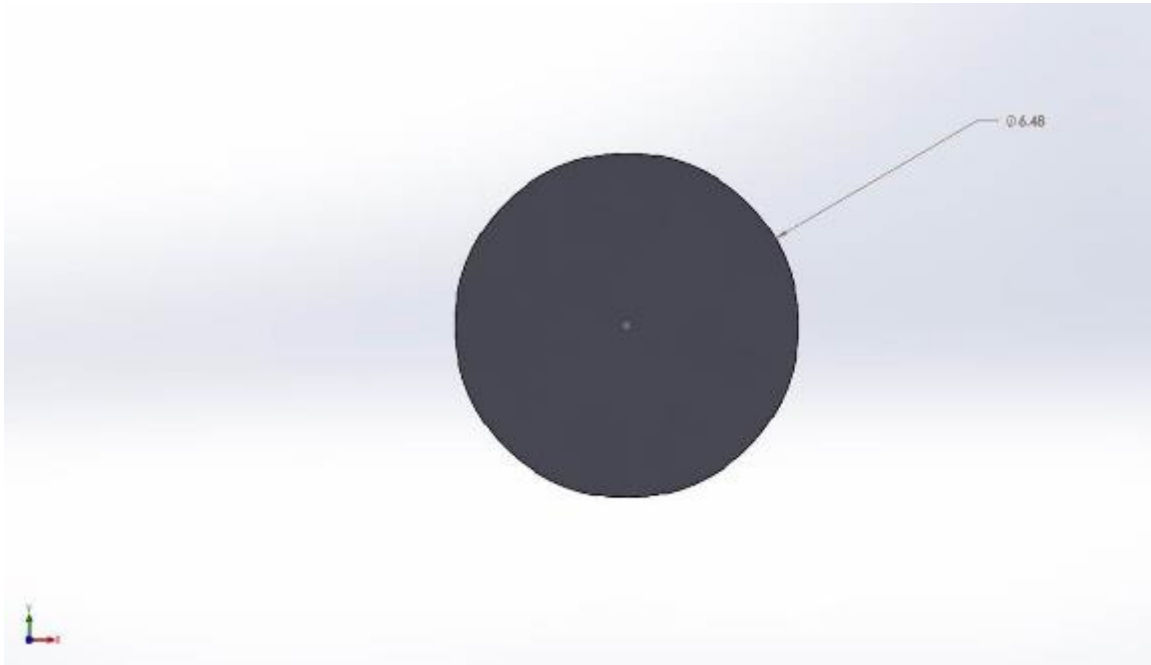


Figure 16. Solidworks image for initial inner rod

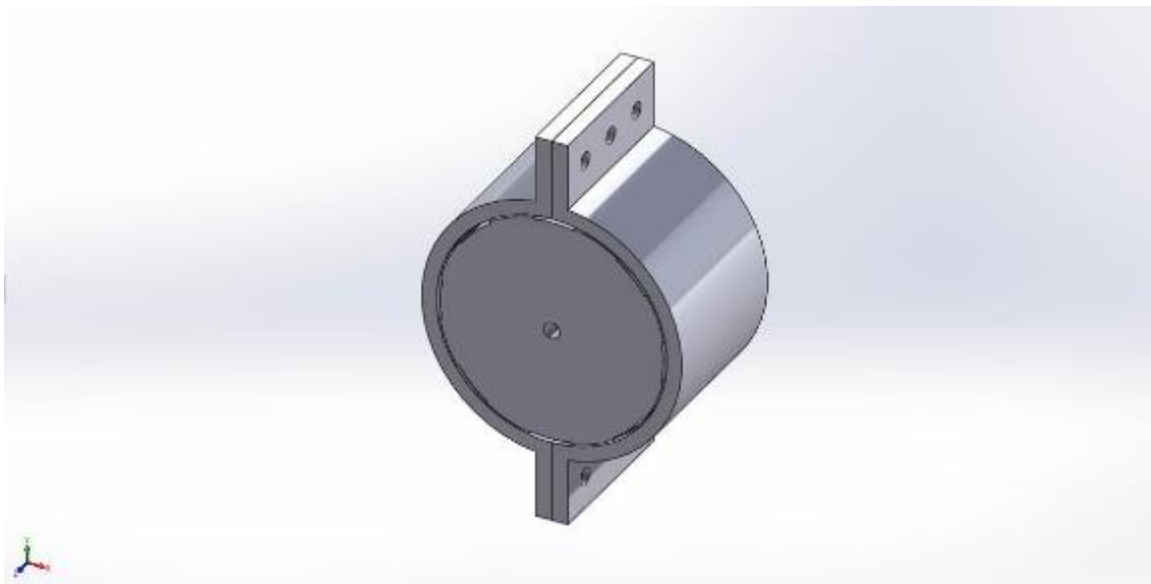


Figure 17. Solidworks image for initial design assembly.



Figure 18. 3D printed model for first design's inner rod.



Figure 19. 3D printed model for first design's outer shell.

The second design increased the diameter for the inner rod to 6.97 cm. This was determined through the size of the circumference, which was the size of the sum of the tape width plus one-mm spacing times 16 (number of strips of tape multiplied by 2). The outer shell also had indents, as shown in Figure 20, which acted as guides to cut the copper tape into the proper size. At the time, there was no known method to properly cut the copper foil tape into the proper shape accurately.

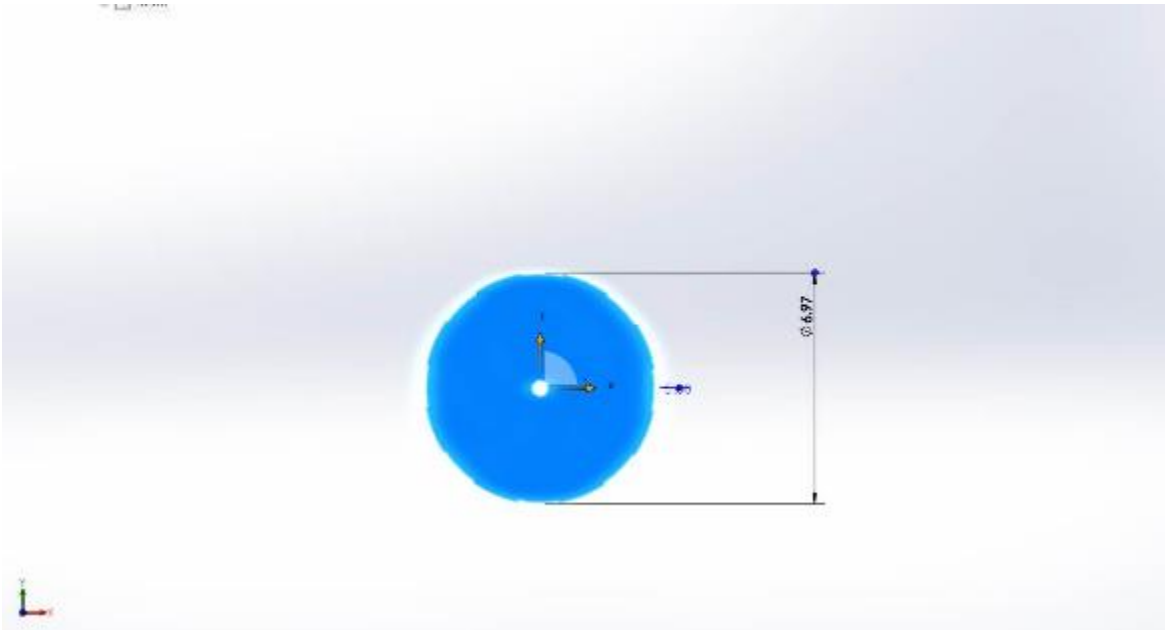


Figure 20. Solidworks design for with new diameter for the inner rod.

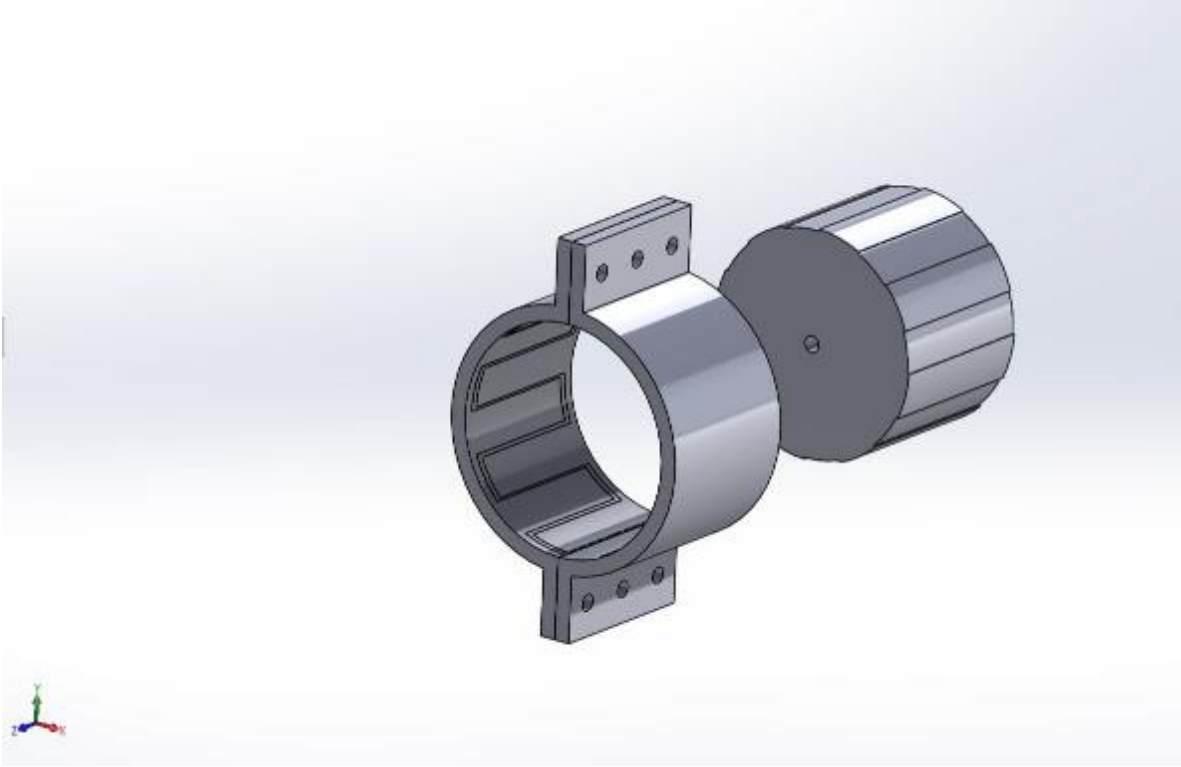


Figure 21. Solidworks assembly for the second design.

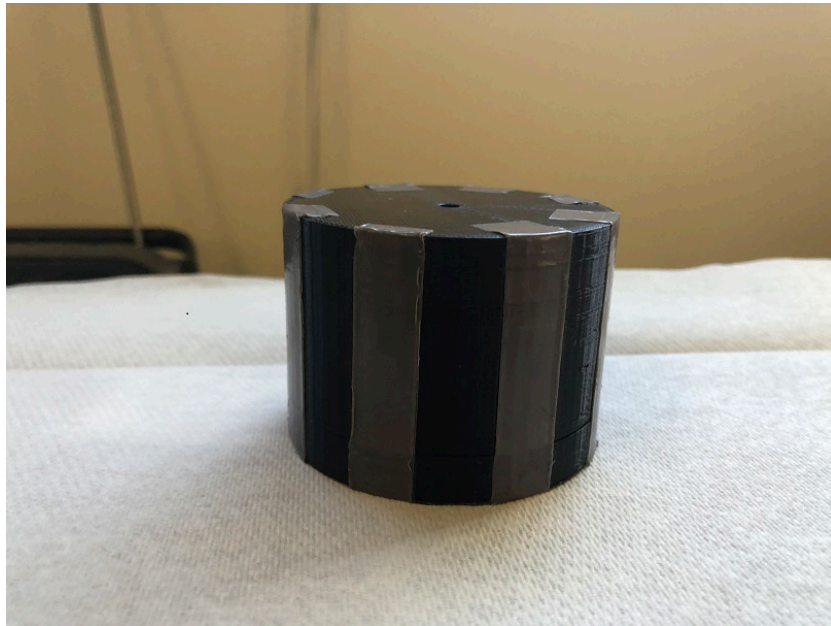


Figure 22. 3D printed model of inner rod for second design.

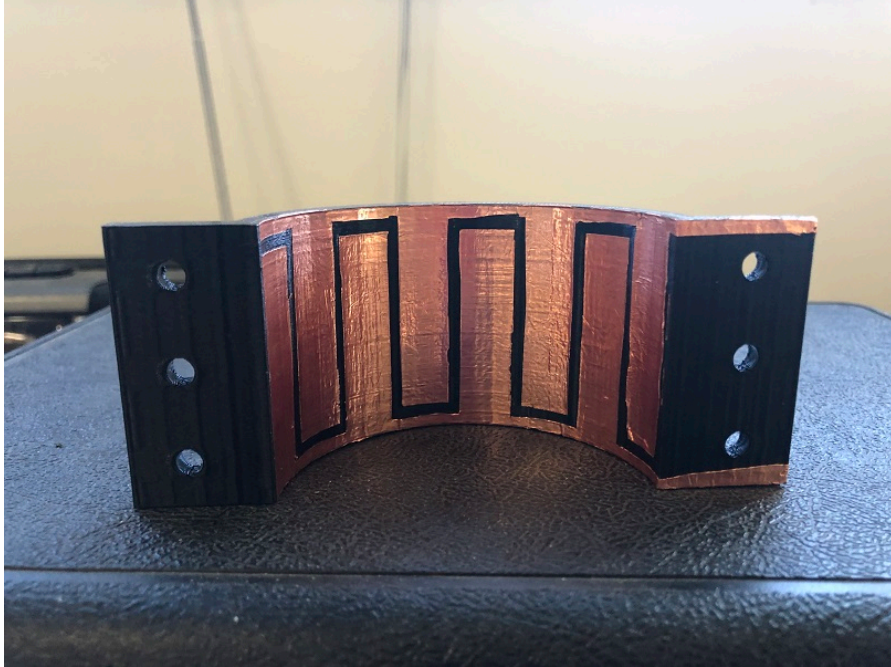


Figure 23. 3D printed model for outer shell for second design.

The second design has several issues. The first is it is difficult to print the outer shell accurately using a 3d printer. The guides were rounded after printing, which made shaping the copper foil tape difficult. The major design flaw was the inner rod was not able to even spin freely with the shells because the indents for the inner rod would catch on the shell. The indents were also too deep causing the inner rod to make no contact with the outer shell.

The size for the third design remained the same. The guides were removed from the previous design, which led to finding a method to cut the copper foil tape accurately and repeatably. The Cricut die-cutter became a viable option for cutting the tape. After making the templates, shown in Figures 24 and Figure 25, the cutter shaped the foil tape accurately and repeatably.

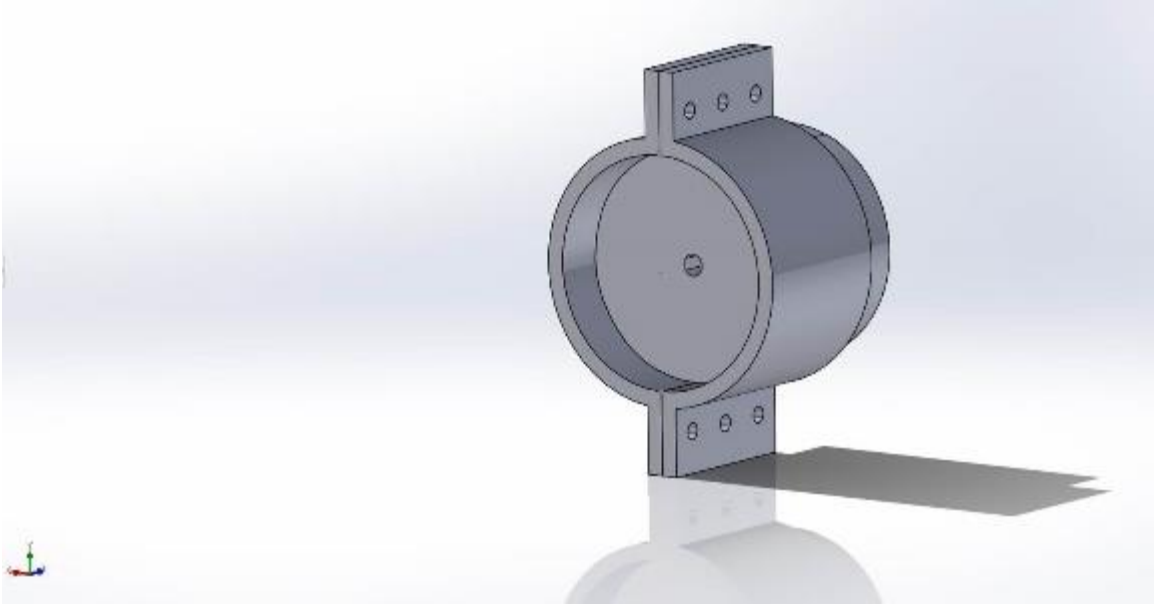


Figure 24. Solidworks assembly for third design.

Figure 25 shows the 3D printed assembly for the third design. The major problem with the third design was prone to defects during the printing process. Since the outer shell was very thin, it became very susceptible to warping, which made it difficult for the inner rod to spin freely inside the shell. The other issue with this design was its difficulty to mount to a rig, which led to the final and improved fourth design.



Figure 25. 3D printed assembly of third design with electrodes.

The final design is a modified version of the third design. The shell is thicker to prevent warping and gap in the bottom is to allow the PLA to bend. It was later discovered that the spacing in the bottom did not add anything to the design due to the stiffness in the PLA. Figure 26 shows the new design for the inner rod. This design removes the grooves along the side to allow testing for various PTFE tape widths.

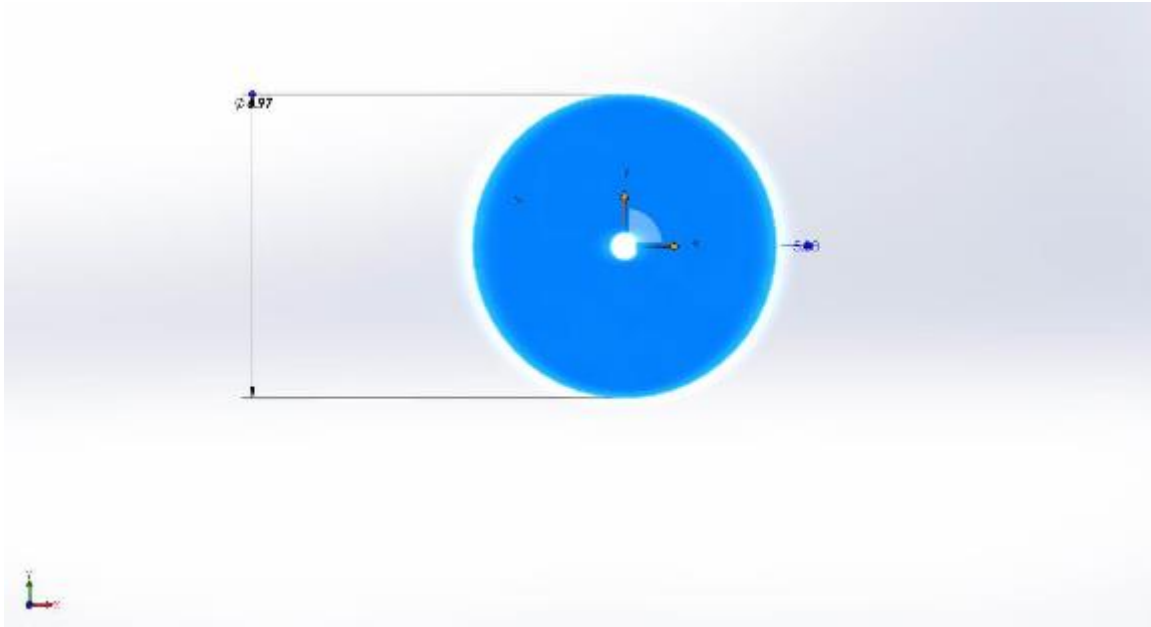


Figure 26. Solidworks design of the final design for the inner rod.

The holes on the top of the TENG, shown in Figure 27, allow screws to fasten it to a rig. The common issue with all the designs was to have the inner rod freely spin inside of the shell. To mitigate this issue, rescaling the rod's size in the 3D printing software by 1% corrected this issue and allowed it to spin within the rig.

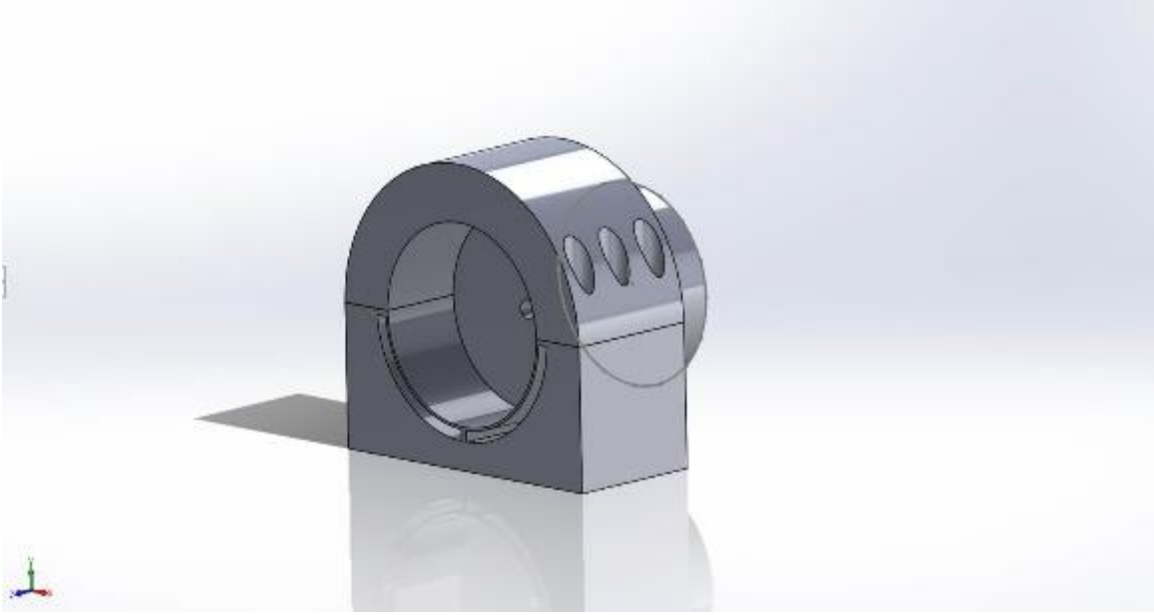


Figure 27. Solidworks assembly of the final TENG design.



Figure 28. 3D printed assembly of final TENG design.

The copper tape used for the electrodes is 5 cm (2 in) wide and cut to shape to use for the electrodes. To ensure accurate and precise cuts, the copper foil tape was cut using a vinyl cutter with a template. The vinyl cutter is a Cricut Maker and the templates were drawn on the Cricut Design Space application. Figures 29 and 30 demonstrate the different sizes for the electrodes used in the different TENG designs. The left design in Figure 8 is the first design tested to demonstrate and develop the TENG. This design did not have enough spacing between the teeth to match the spacing for the PTFE tape and copper tape overlapped with other electrode. Figure 29 shows the initial and improved design to match the spacing for the inner rod. Figure 30 shows the various sizes tested. The 3 mm fingers are to match sizing of the previous NPS design.

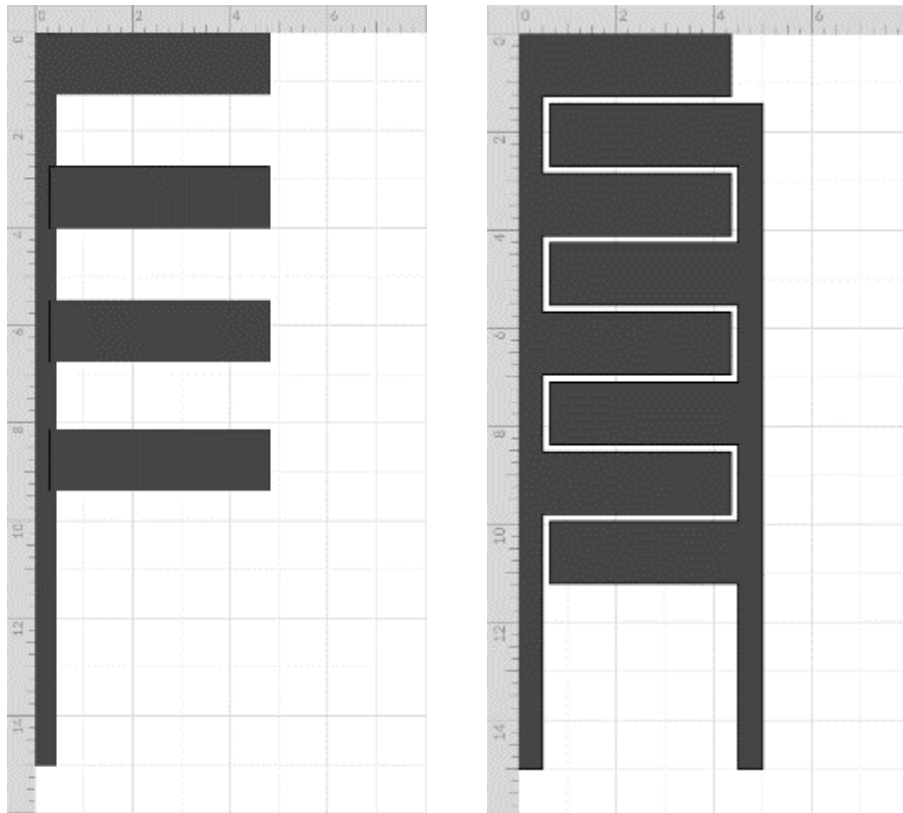


Figure 29. Design for TENG electrode tracks with 1.27 cm ($\frac{1}{2}$ in) fingers.
(Left) Initial design (right) improved design.

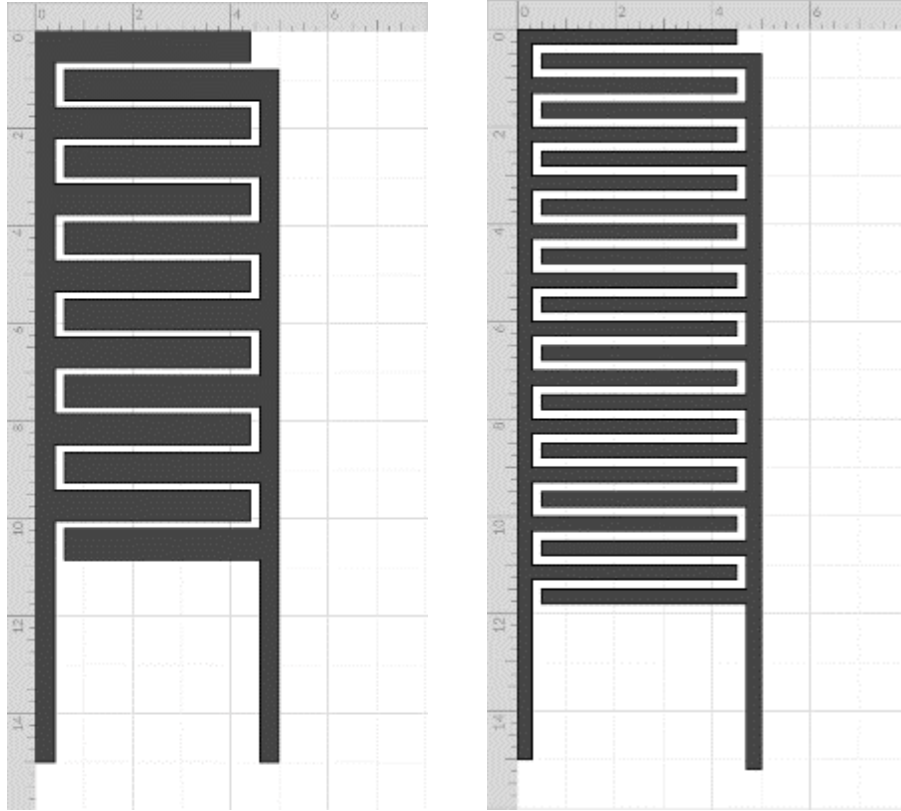


Figure 30. Design for TENG electrode tracks at (left) 0.635 cm ($\frac{1}{4}$ in) and (right) 3 mm fingers.

Table 1. Surface area for electrode and spacing between fingers for one half of the TENG.

Electrode (one half)	Surface area (cm ²)	Remaining area (cm ²)
Initial Design	51.672	3.305
1.27 cm fingers	53.406	1.571
0.635 cm fingers	47.244	7.734
0.3 cm fingers	36.63	18.348

The surface remaining area is determined by the inner diameter of the outer shell, 7 cm. Using the formula for area of a cylinder, the total area is equal to 54.978 cm².

Subtracting this area with the surface area of the electrodes will give the remaining area or “empty space” in the inner shell of the TENG.

Table 2. Surface area of the combined halves of the TENG.

Electrode (both halves)	Surface area (cm ²)	Remaining area (cm ²)
Initial Design	103.344	6.61
1.27 cm fingers	106.812	3.142
0.635 cm fingers	94.488	15.468
0.3 cm fingers	73.26	36.696

D. DESIGN CHALLENGES

The inner rod needs to fit in the shell with minimal spacing in order to provide enough contact between the PTFE and copper electrodes, which is one reason why the outer shell is separated into two pieces. Even with the two parts, it is difficult to have perfect spacing. TPU was an alternative material for the outer shell due to its flexibility, but because it is a difficult material to print. Another mitigation was to add springs between the top and bottom half. This method was not used because it would add more complexity to the build. The simplest and effective solution was to shrink the inner rod during the printing process. This prevented overcomplicating the TENG design and simplifying the manufacturing process.

THIS PAGE INTENTIONALLY LEFT BLANK

III. EXPERIMENTATION PROCESS

A. TRANSLATIONAL MOTION TENG (NPS MODEL)

The previous NPS model is designed after the NASA Ames model, which demonstrates translational motion to produce the triboelectric effect [6, 9, 10]. The initial design for the TENG is mounted to an oscillating column (OC). The interdigitated electrodes consist of copper. Each finger is 3 mm wide with 1.5 mm spacing and soldered wires on each electrode to gather readings for voltage and current. The surface area for the electrodes is 2.118 cm² [9].

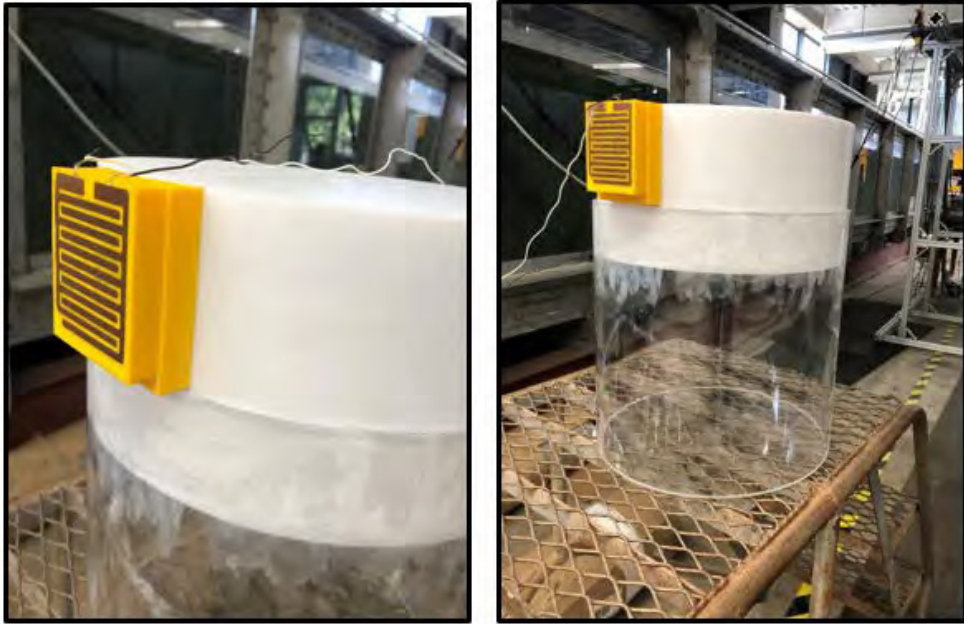


Figure 31. First NPS TENG model. Source [9].



Figure 32. Final assembly of initial NPS TENG model. Source [9].

The first experiment, conducted by Reilly [9], utilized direct wave motion to produce the sliding for the TENG. This experiment gathered voltage data from the sliding motion. The design is a simple design, however is limited to the oscillating motion from the wave tank.

The second experiment, conducted by Mann [10], improved the original NPS model by utilizing a pulley system and the motion from the OC to drive the TENG. Figure 33 shows a schematic of the change. The spring acts as a damper for the TENG and OC, which allow the TENG to fluctuate with the wave motion. The experiment also had a section that

utilized gear ratios, to increase the frequency for the TENG and in turn increases the power output for linear motion.

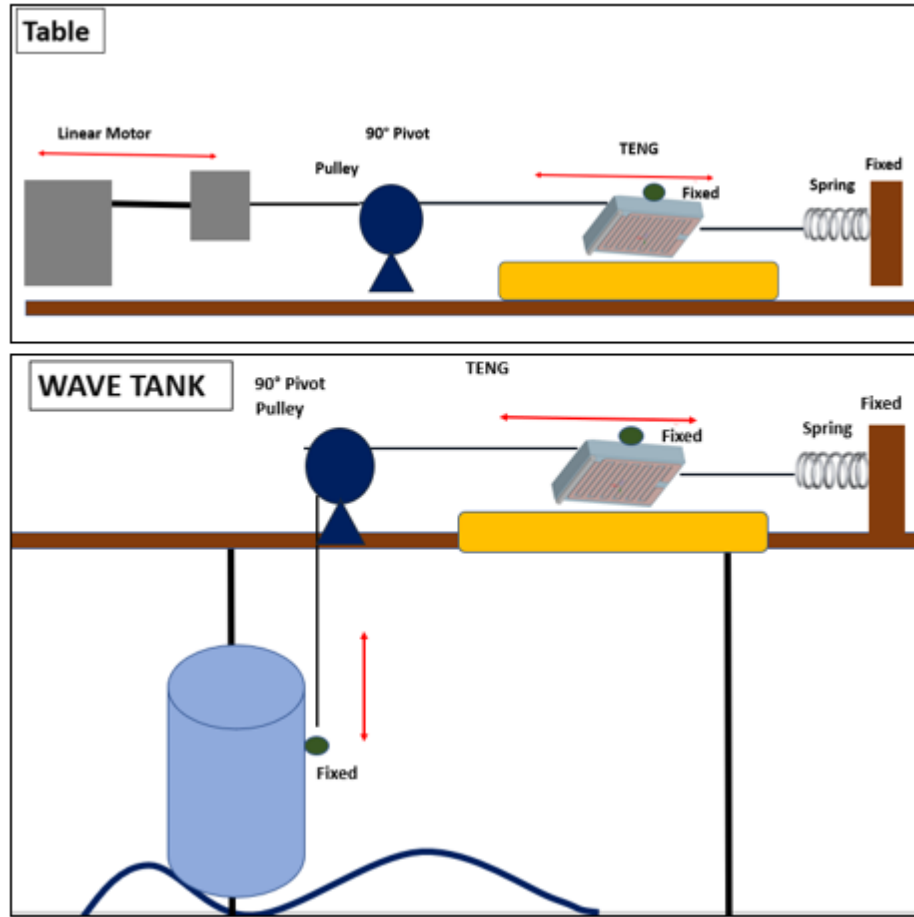


Figure 33. Schematic of second version of NPS TENG model. Source [10].

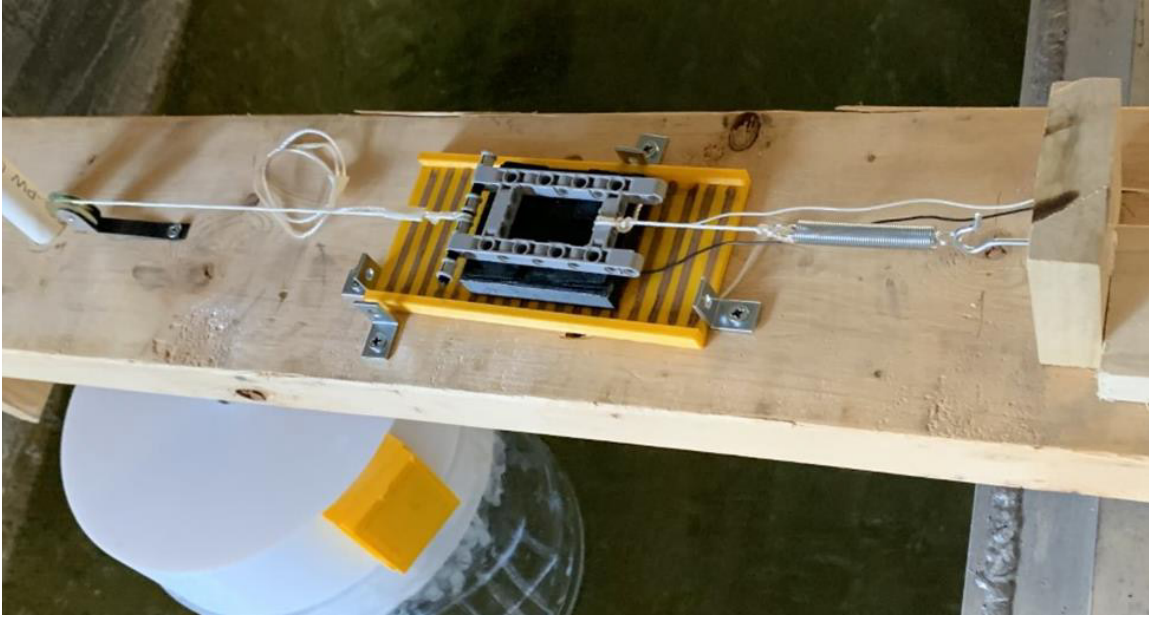


Figure 34. Final assembly of second NPS TENG. Source [10].

This design had similar problems as the initial experiments in that the low frequency produces a minimal amount of power. As shown in Figure 35, the new design has a low power density. The voltage is significant; however, current is in the magnitude of nanoamps.

B. ROTATIONAL TENG PROCESS

This testing is very similar to previous NPS experiments with TENG. The setup utilizes a direct current (DC) motor vice a linear reciprocating motor. The tests consist of running the motor to spin the inner rod at various revolutions per minute (RPM). The motor for this experiment is a Greartisan 12 V 550 RPM. A variable motor controller connects to the motor to regulate the speed.



Figure 35. DC motor drives inner rod for TENG.

A digital laser tachometer, Figure 36, ensures proper control for the motor speed. As shown in Figure 33, the reflective tape on the inner rod ensures the tachometer gathers the proper reading for the TENG. There is a power loss in the motor due to friction; therefore, the motor spins the inner rod for the TENG spins at a maximum of 500 RPM.



Figure 36. Digital tachometer.

Figure 38 shows the electrode with its leads. This design facilitates connecting the leads to the TENG to gather readings without soldering wires. Previous designs determined soldering to the copper foil is possible, however adds an unnecessary and difficult step. Soldering the wire to a thin strip of copper tape is not ideal and once attached, becomes an easy target for rips and tears along the foil. Securing the wires between the upper and lower half of the TENG speeds up the connection process and facilitates replacing a damaged TENG or electrode. Figure 37 shows the wire connections to the TENG. Once the TENG is bolted, it secures the wire connections, allowing accurate readings.



Figure 37. TENG assembly with wires attached to electrodes, and reflective tape for tachometer.

Figure 38 shows the electrodes attached to the TENG bracket. The electrodes have leads on one side, and when connected, enhance the surface area for the TENG.



Figure 38. Top view of TENG with electrodes and lead.

Figure 39 shows the load attached to the TENG to read it with the Tektronix TCPA300 amplifier shown in Figure 40.

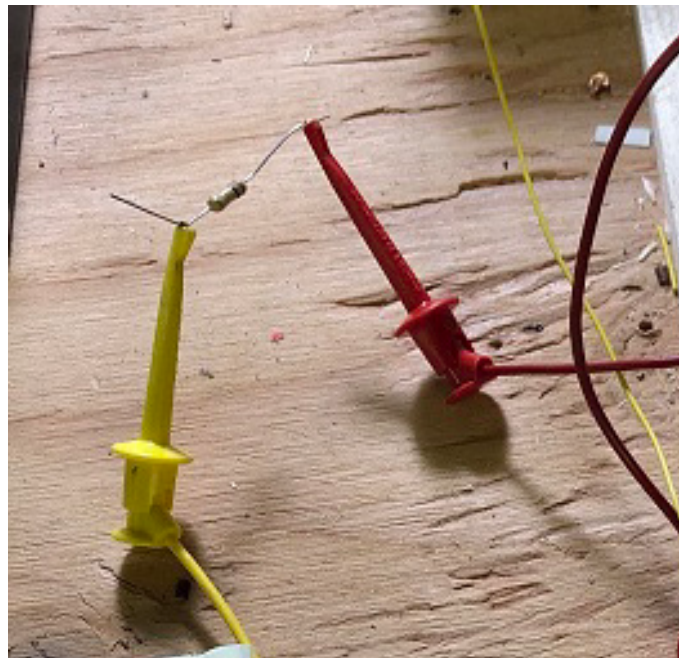


Figure 39. Load attached to TENG to gather current readings.

The test for the TENG is to conduct initial runs for each of the improved electrode sizes at 60, 120, 240, and 360 rpms without a load to gather the initial voltage reading. Upon completing the readings, a load is attached to the TENG to observe current and any changes that may occur due to the new load. The readings are then measured at the same rpm as the test with no load, 60, 120, 240, and 360 rpms. The current is gathered from a probe attached to a Tektronix TCPA300 amplifier and displayed on the Tektronix MSO Mixed Signal Oscilloscope shown in Figure 41. The final test is to attach two TENGs in series to determine if there is any change increase in current.



Figure 40. Tektronix TCPA300 amplifier connects to the TENG and oscilloscope.

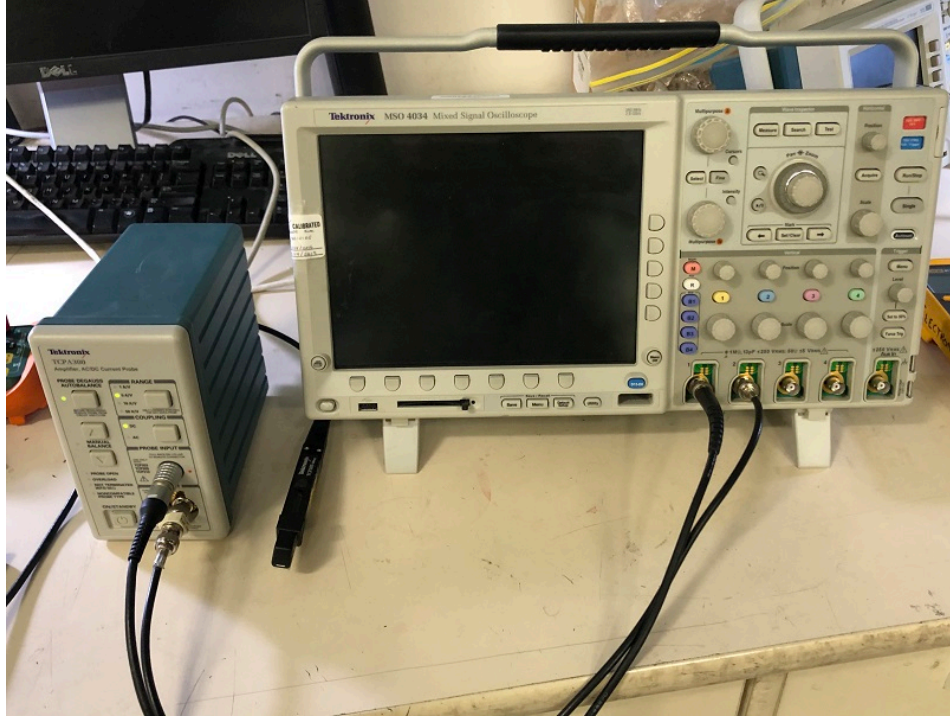


Figure 41. Amplifier attached to Tektronix MSO 4034.

If there are issues with gathering current readings, the Keithley 617 Electrometer is the secondary equipment. The Keithley 617 is a more sensitive tool to measure current and can gather readings in the picoamps. Mann [10] utilized the Keithley 617 to collect data. The electrometer is a secondary means to measure because it is outdated. It does not have conventional means to extract data like modern electrometers and oscilloscopes. Figure 42 is a picture of the device. Figure 43 shows how to connect the leads to the electrometer. The red clip connects to one terminal, while the black connects to another. The green clip is used if the circuit needs shielding and would connect to the outer shell. It is not necessary for these tests. The Keithley 617 has an internal load, so it is not necessary to attach a load to gather readings for current.



Figure 42. Keithley 617 Electrometer.

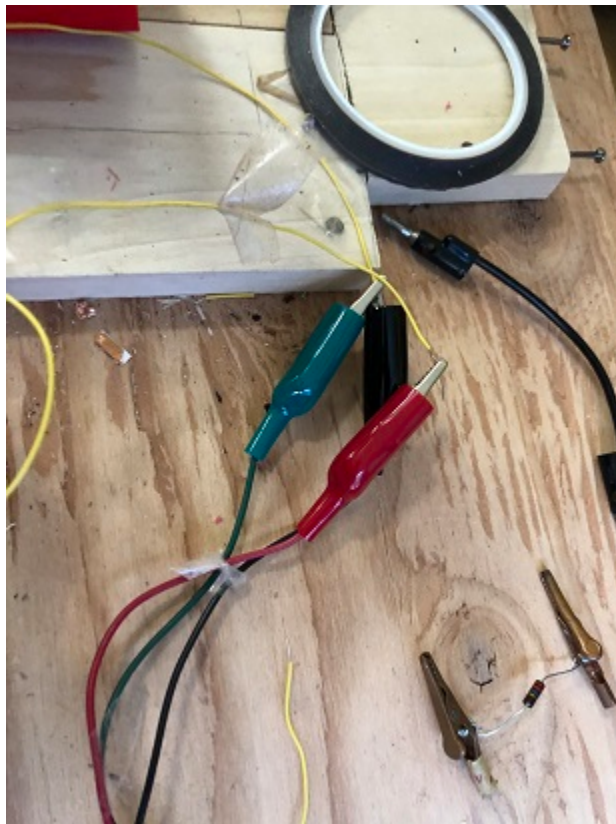


Figure 43. Lead connections from the TENG to the electrometer.

There is a wooden rod that connects the two inner rods to ensure the two spin at the same speed as shown in Figure 44. This figure also shows the wires connecting the TENG in series.

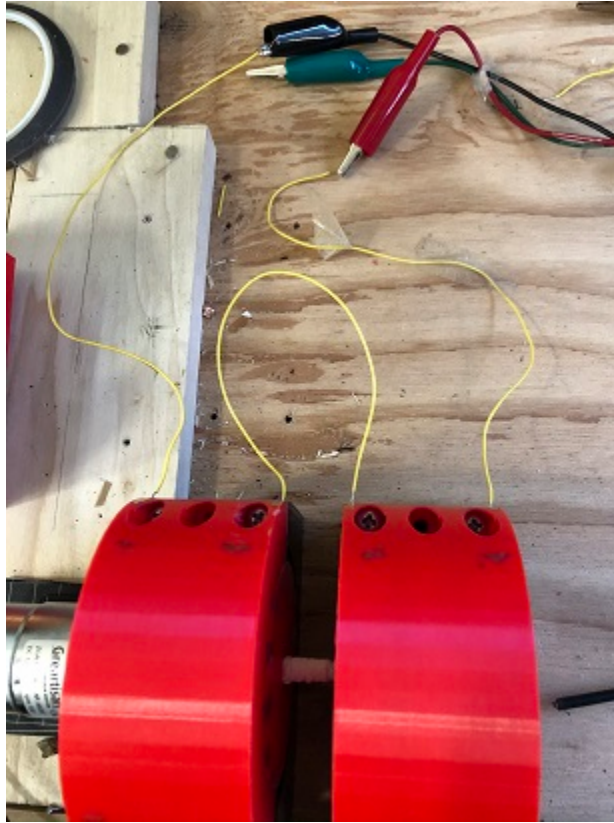


Figure 44. Two TENGs connected in series.

Figure 45 shows connecting the TENG in parallel. The two TENG with the most optimal performance are used for series and parallel connection.

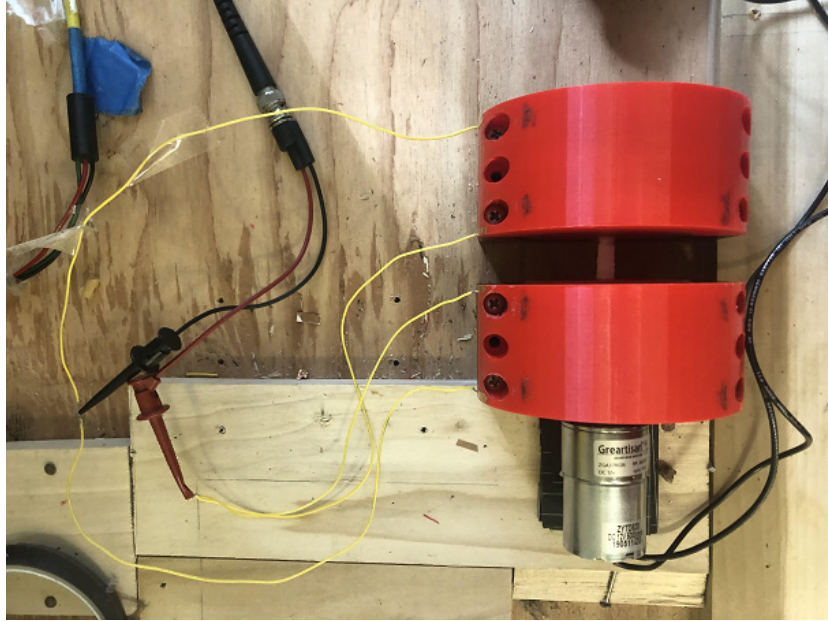


Figure 45. Connecting TENG in parallel.

Each size of TENG is labeled a number. TENG 1 is the 1.27 cm ($\frac{1}{2}$ in) electrodes. TENG 2 is the 0.635 cm ($\frac{1}{4}$ in) electrodes. TENG 3 is the 3 mm electrodes. TENG 4 is connecting two TENG in series. TENG 5 is connecting the TENG in parallel.

THIS PAGE INTENTIONALLY LEFT BLANK

IV. RESULTS AND DISCUSSION

There were three different sizes for electrodes for the TENG and the motor ran at four speeds: 60, 120, 240, and 360 rpms. The tests consisted of a total of 16 experimental runs, which included connecting two TENGs in series. The TENG had the motor directly connected to the inner rod and did not take gear ratios into consideration.

The Tektronix MSO 4034 gathered the voltage information for the experiment. There was no issue with gathering the voltage readings with the TENGs. Since current is in the nanoamps, the Tektronix TCPA300 amplifier was not the proper choice to gather data, it was necessary to switch to the Keithley 617. This equipment is very limited in exporting data, but very accurate in reading very low current. The current test ran for 20 seconds with 60 data points.

Power is equal to the product of voltage and current. Power density is determined by dividing the power by the area of the electrodes.

A. TESTING TENG INDIVIDUALLY

1. Experimental Results for TENG 1

a. *Voltage Data*

The Tektronix MSO 4034 gathered voltage data and was set to 1 sample/200 milliseconds. The total number of data points for each voltage is 1000 samples. Figure 46 shows the maximum voltage vs the speed for TENG 1.

As shown in Figure 46, the average voltage increases as the speed increases. This confirms the conclusion determined by Reilly [9] and Mann [10] that the frequency of contact between the copper electrode and PTFE tape are therefore proportional to the power output.

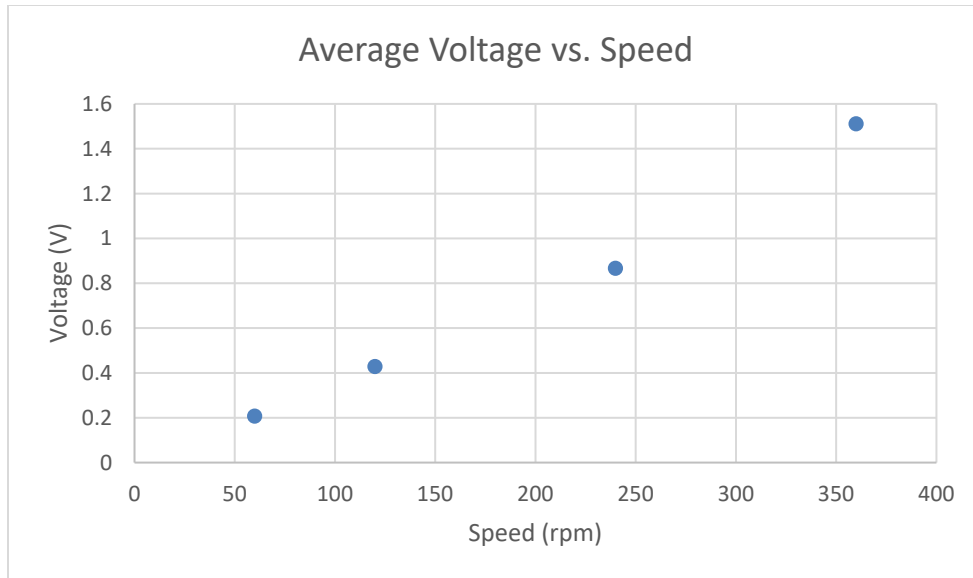


Figure 46. Average voltage data for TENG 1.

b. Current Data

As stated earlier, TENGs do not produce sufficient current alone, which is why they are typically added connected in series or parallel to amplify the power output into something useable. Figure 47 shows the average current for TENG 1. Notice the current is low and in the nanoamps and how the current does not steadily increase with speed. This inconsistency demonstrates how unstable TENG 1 is.

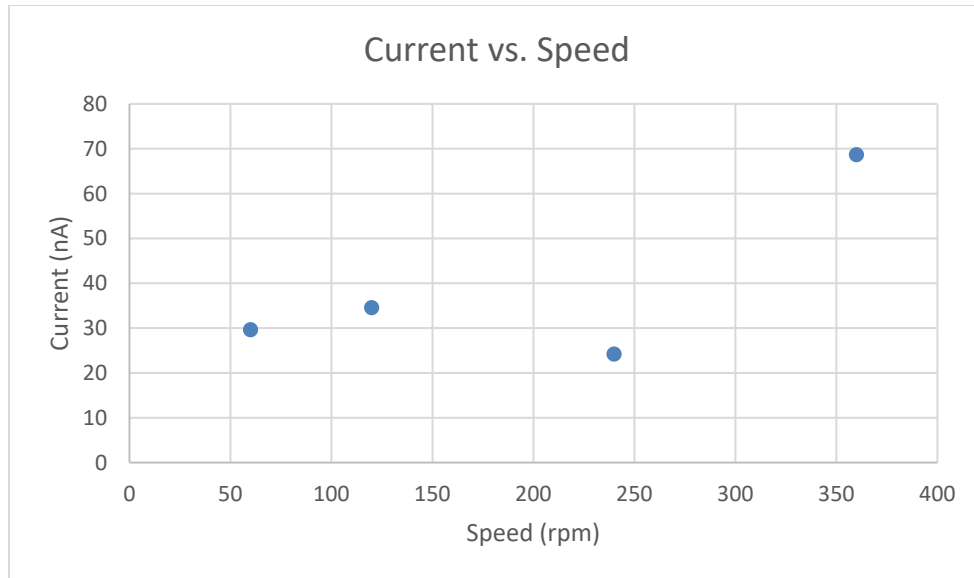


Figure 47. Average current for TENG 1.

c. Power Density Data

Power is calculated using the average voltage and current. The power density is calculated by dividing the result by the contact area of the electrode. TENG 1 has the largest contact area of the individual TENGs. Figure 48 displays the power density for TENG 1. Since the current is not stable, the power and power density are also unstable.



Figure 48. Power density for TENG 1.

2. Experimental Results for TENG 2

a. Voltage Data

TENG 2 produced similar results as TENG 1 because the voltage is directly proportional to the speed. Figure 49 shows the average voltage for TENG 2. TENG 2 performed more poorly than the thicker electrodes, however, as discussed later, it produces a more stable power.

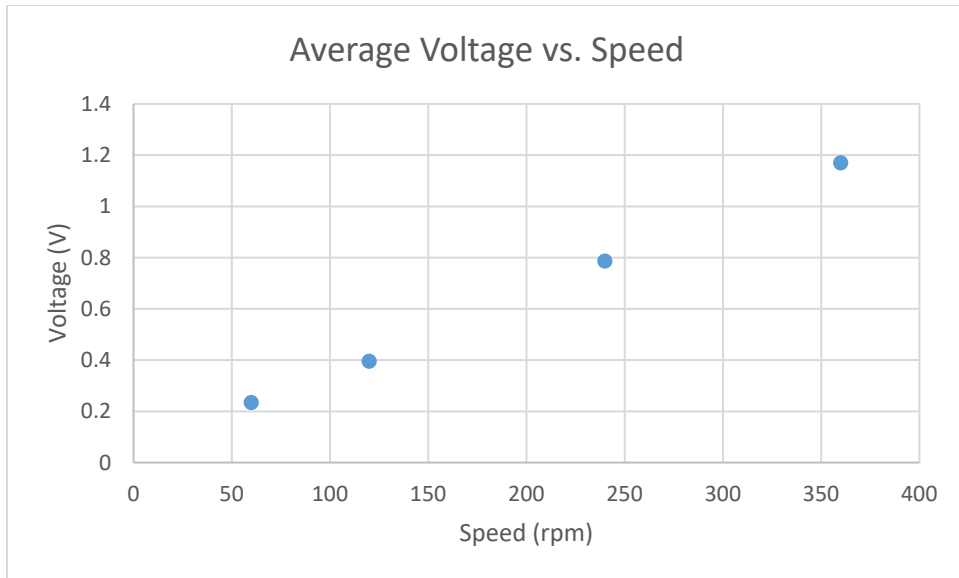


Figure 49. Average voltage data for TENG 2.

b. Current Data

The current for TENG 2 is more consistent than TENG 1. As displayed in Figure 50, the current is linearly increasing with the speed. TENG 2 demonstrates the normal pattern for TENG, where current increases with speed. At the lower speeds, 60 and 120 rpm, the current is unstable.

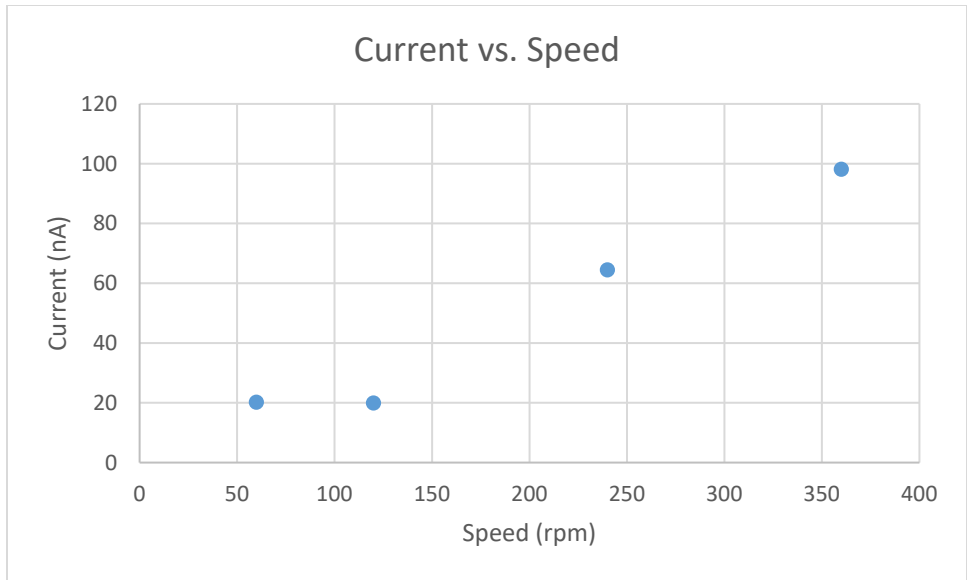


Figure 50. Average current for TENG 2.

c. Power Density

As illustrated in Figure 51, the power density increases with speed, since the power density is a function of the voltage and current.

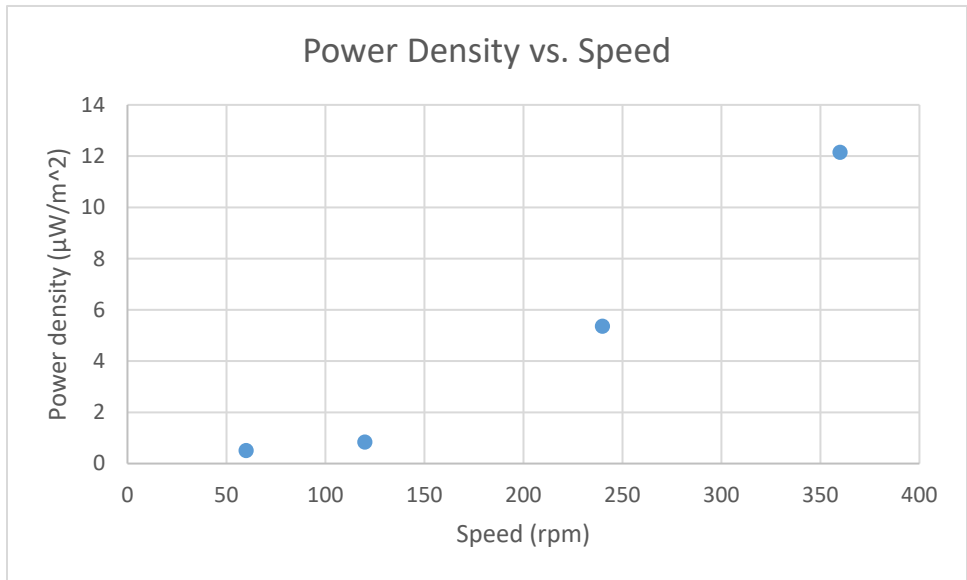


Figure 51. Power density for TENG 2.

3. Experimental Results for TENG 3

The width of the interdigitated fingers for the electrodes used for TENG 3 emulates the previous NPS TENG designed by Reilly [9]. The width for the fingers is 3 mm with an increased spacing of 2 mm. The increased spacing facilitated applying the copper tape to the TENG.

a. Voltage Data

Figure 52 shows the average voltage for TENG 3. The average for the voltage output for this TENG is not much higher than TENG 1.

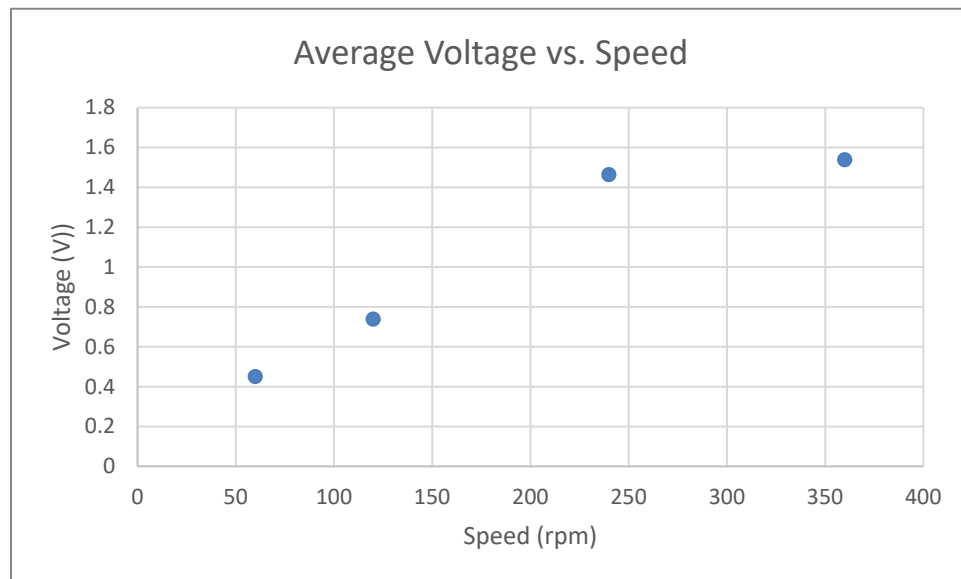


Figure 52. Average voltage for TENG 3.

b. Current Data

Figure 53 shows the current data for TENG 3. Similar to previous data, the current is directly proportional to the TENG's speed. This size of TENG has the most optimal current output of all the individual TENGs. The current for TENG 3 is stable at lower speeds, resulting in a higher variable for speed that the TENGs can operate. This can be attributed to the smaller fingers, which increase the number of interdigitated fingers,

resulting in a higher contact frequency. A higher contact frequency results in a higher power output.

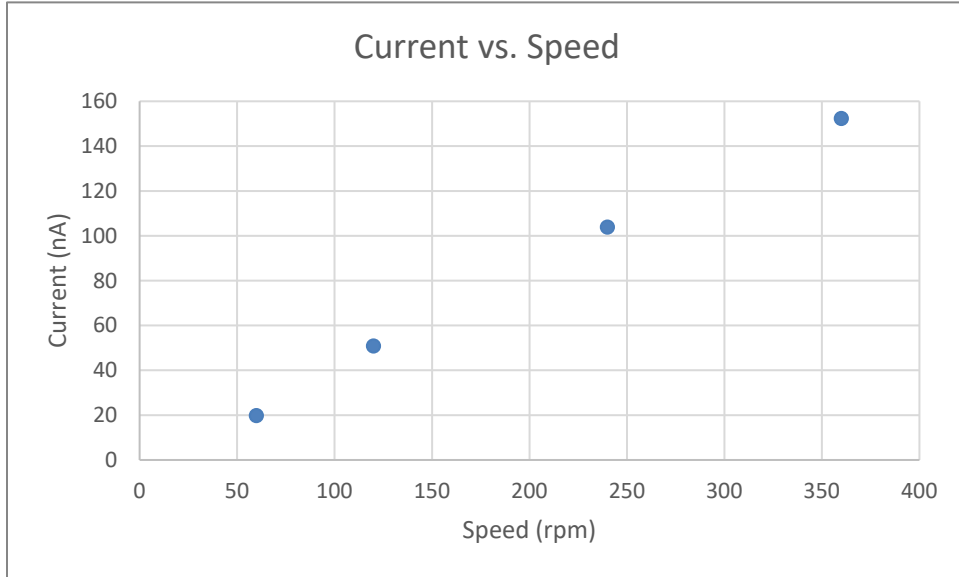


Figure 53. Average current for TENG 3.

c. Power Density Data

Figure 53 shows the power density for TENG 3. The contact area for this TENG is the lowest and it has the highest average current output for the varying speeds. This results in producing the highest power density of the individual TENGs. TENG 3 has the smallest surface area for the electrodes of the 3 individual TENG. Since it has the highest current reading of all the TENG and smallest area, it has the highest power density. As stated earlier it can be attributed to the increased number of interdigitated fingers that increase the contact frequency between the copper electrode with PTFE tape.



Figure 54. Power density for TENG 3.

B. TESTING COMBINING TENG (SERIES AND PARALLEL)

1. Experimental Results for TENG 4

TENG 2 and TENG 3 had the most optimal results of the three individual TENGs and were selected to combine into series for tests. TENG 4 is connecting TENG 2 and TENG 3 in series.

a. Voltage Data

Figure 55 displays the current data for TENG 4. The voltage is directly proportional to the speed. As expected, the average voltage for the TENG 4 is higher than the individual TENG.

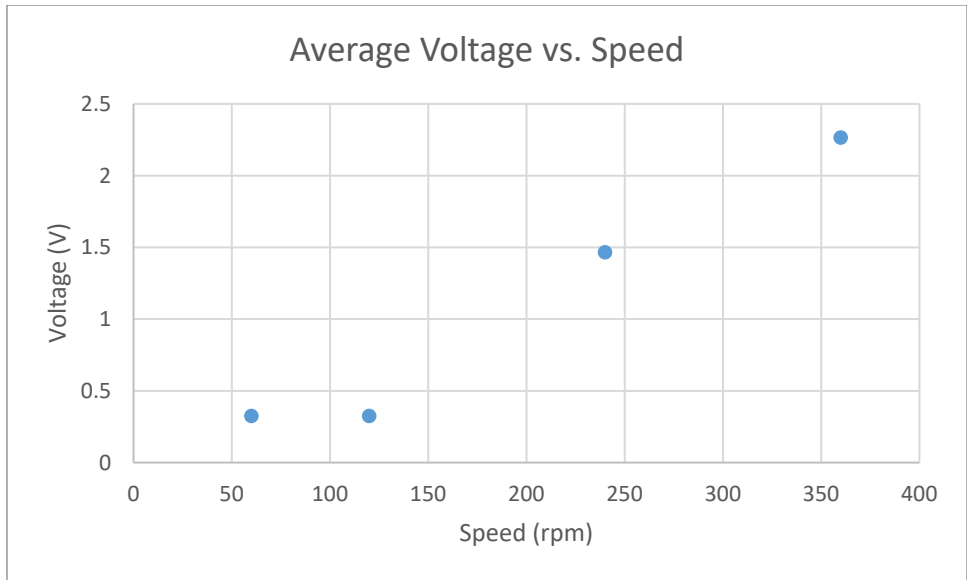


Figure 55. Average voltage for TENG 4.

b. Current Data

Figure 56 shows the current data for TENG 4 at variable speeds. The current increased from TENG 3, however, it is a nominal difference.

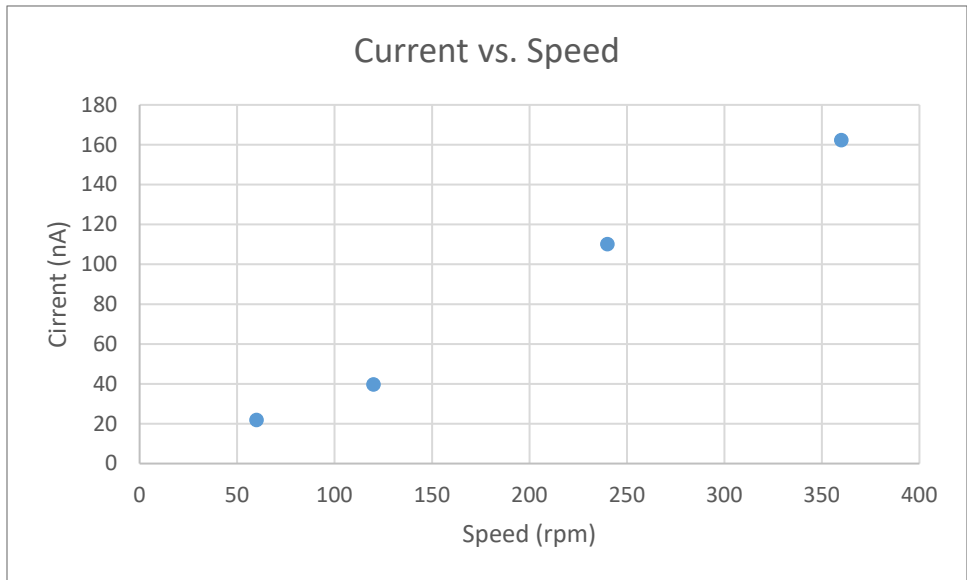


Figure 56. Current for TENG 4.

c. Power Density Data

Figure 57 shows the power density data for TENG 4. Despite producing the highest power output than the individual TENG, the contact area for the electrodes reduces the power density and makes it pale in comparison to TENG 3.

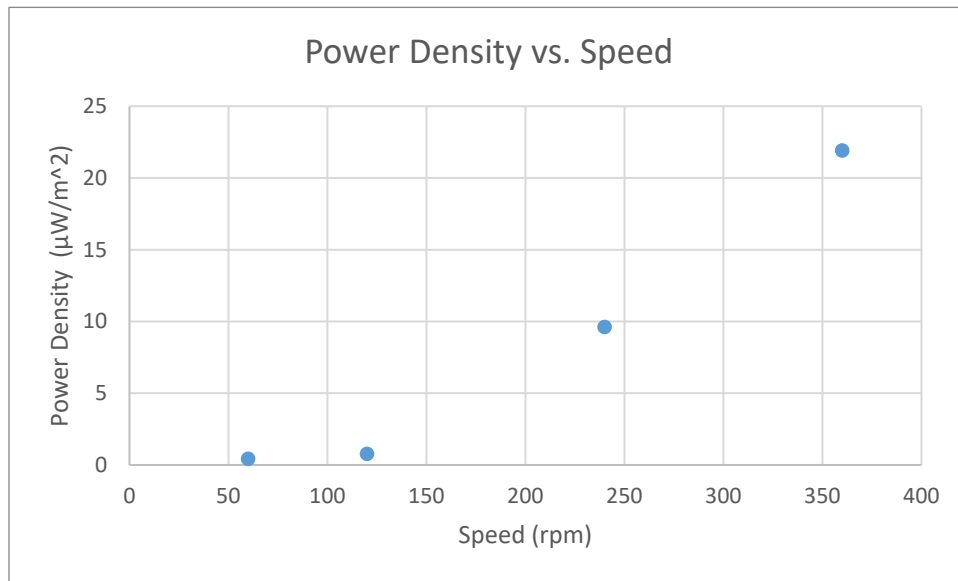


Figure 57. Power density for TENG 4.

2. Experimental Results for TENG 5

TENG 5 combines TENG 2 and TENG 3 in parallel to determine the output and determine if the settings are optimal.

a. Voltage Data

Figure 58 displays the average voltage output for the TENG. Despite being in parallel, TENG 5 has a higher voltage output than TENG 4.

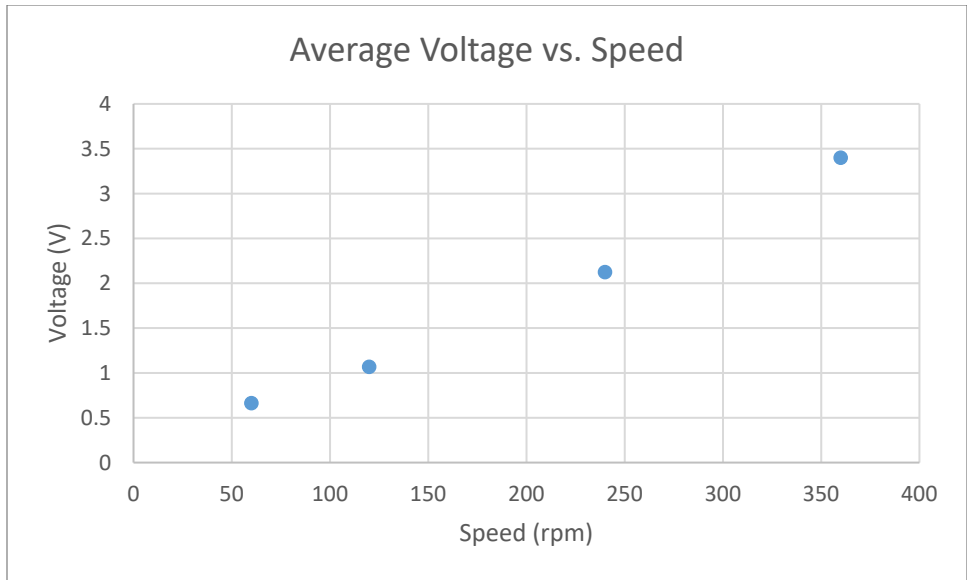


Figure 58. Average voltage for TENG 5.

b. Current Data

The average current for TENG 5 increased from TENG 4 through connecting them in parallel as displayed through Figure 59. TENG 5 produces much higher current outputs at lower speeds than the other TENGs.

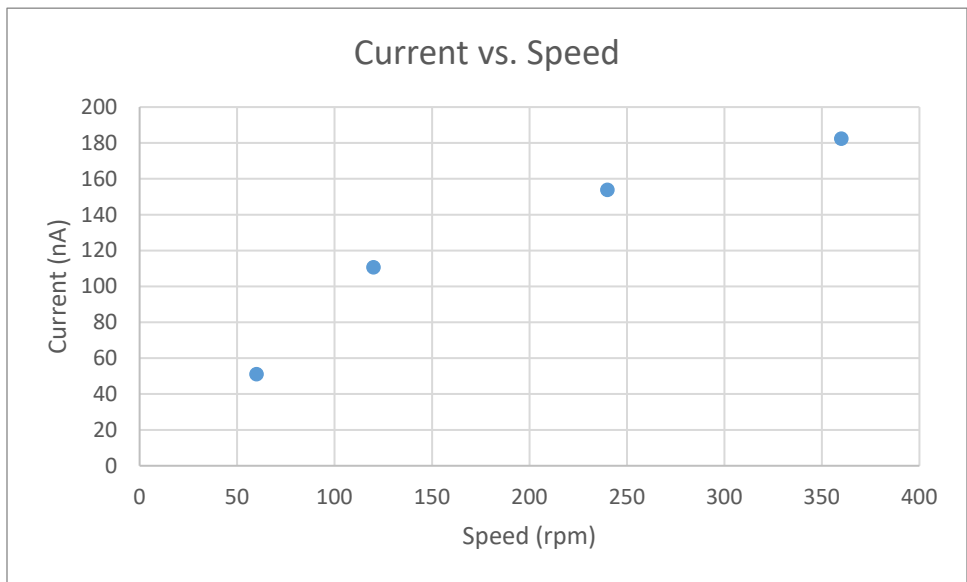


Figure 59. Average current for TENG 5.

c. Power Density Data

Since the voltage and current are the highest of all the TENG in this experiment, this TENG produces the highest power output. Figure 60 shows the power density for TENG 5. Despite having a high contact area for the electrodes, TENG 5 also produces

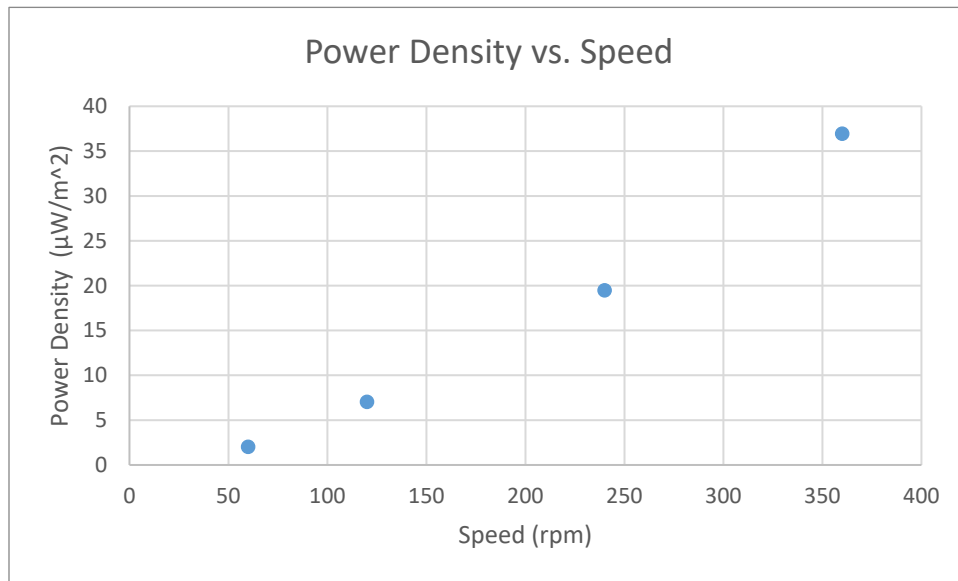


Figure 60. Power density for TENG 5.

C. SUMMARY OF ANALYSIS RESULTS

TENG 3 produced the most optimal performance of testing the individual TENGs. TENG 5 produced the most optimal performance for combining the TENGs. The thinner interdigitated fingers allowed more fingers to attach to the TENG 3. This results in more contact frequency between the PTFE tape and copper electrodes, which produces a higher power output. Combining the TENG in parallel for TENG 5 improved the overall performance.

1. Voltage Data

Figure 61 is a plot of the voltages from all the TENG. TENG 5 produced the overall highest voltage output. TENG 3 performed more optimally than TENG 1 at all speeds. TENG 3 also has a greater voltage output at lower speeds, making it ideal to implement

harvesting energy from low frequencies. This increase in voltage is not a major increase and is negligible. Table 3 displays numerical values for the average voltage of all the TENGs.

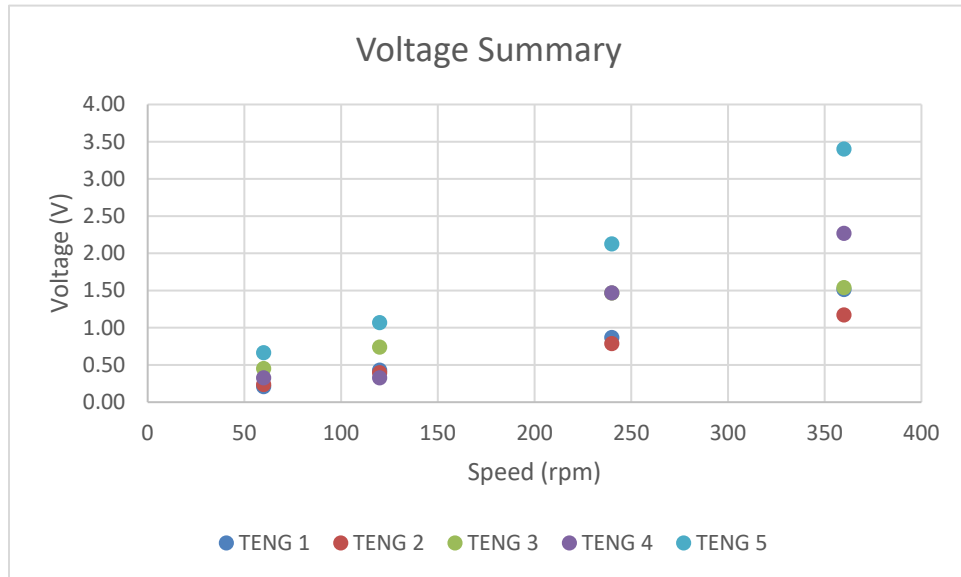


Figure 61. Voltage summary plot.

Table 3. Voltage data (V) summary table.

Speed (rpm)	TENG 1	TENG 2	TENG 3	TENG 4	TENG 5
60	0.21	0.23	0.45	0.32	0.66
120	0.43	0.39	0.74	0.32	1.07
240	0.87	0.79	1.46	1.47	2.12
360	1.51	1.17	1.54	2.27	3.40

2. Current Data

Figure 62 is a summary of the current readings and Table 4 provides the numerical values for the graph. TENG 5 has the highest current output of all the tests. TENG 4's current reading is similar to TENG 3.

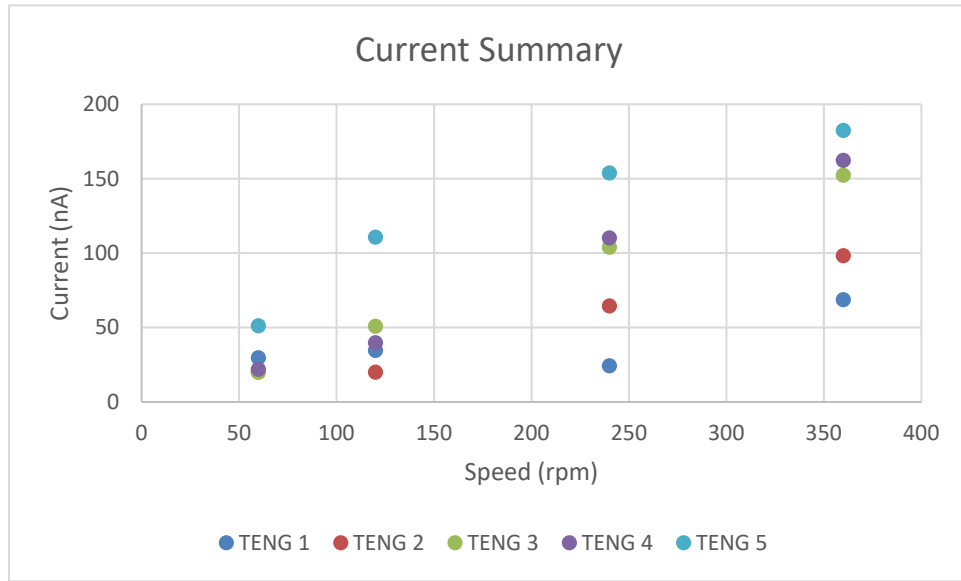


Figure 62. Current summary plot.

Table 4. Current (nA) summary table.

Speed (rpm)	TENG 1	TENG 2	TENG 3	TENG 5	TENG 5
60	30	20	20	22	51
120	35	20	51	40	111
240	24	64	104	110	154
360	69	98	152	162	182

3. Power Density

Figure 63 shows the summary for the power in each TENG with numerical values displayed in Table 5. If the TENG has a high power, it does not mean it will have a high power density. As shown in Figure 64, the power density for TENG 3 is greater than TENG 4. Table 6 displays the numerical values for the power density. The power is found through taking the average of the absolute value of the voltage and multiplying it with the average current.



Figure 63. Power summary.

Table 5. Power (nW) summary table.

Speed (rpm)	TENG 1	TENG 2	TENG 3	TENG 4	TENG 5
60	6.11	4.71	8.89	7.08	33.79
120	14.76	7.85	37.46	12.87	117.94
240	20.95	50.60	151.96	161.27	326.56
360	103.69	114.75	234.11	367.60	619.67

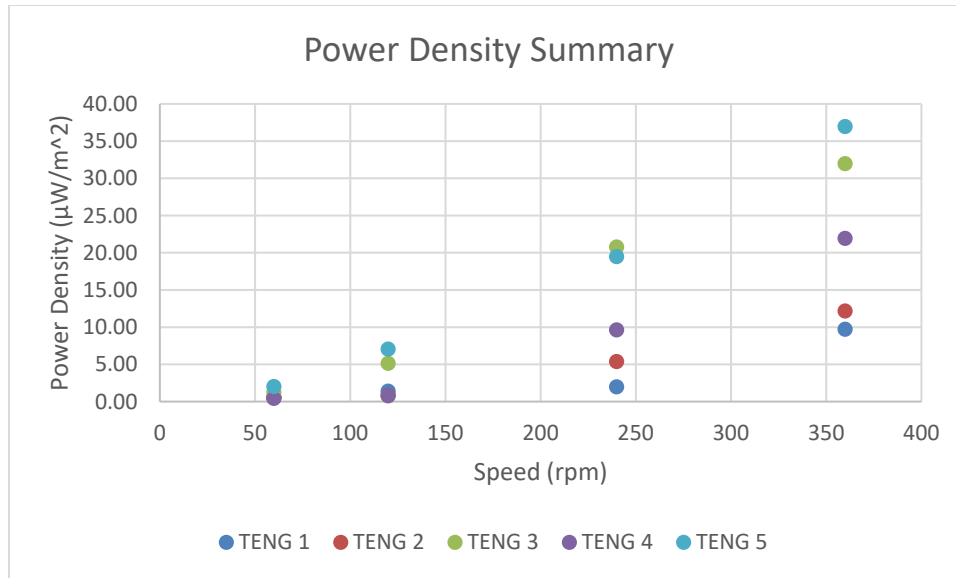


Figure 64. Power density summary.

The power density for TENG 5 is significantly higher and more stable than the individual TENGs.

Table 6. Power density (μW/m²) summary table.

Speed (rpm)	TENG 1	TENG 2	TENG 3	TENG 4	TENG 5
60	0.57	0.50	1.21	0.42	2.01
120	1.38	0.83	5.11	0.77	7.03
240	1.96	5.36	20.47	9.61	19.47
360	9.71	12.14	31.96	21.91	36.94

D. DISCUSSION

The reason for testing three different size electrodes for the TENGs is to determine if the thickness of the electrodes affected the power output. TENG 1, TENG 2, and TENG 3, are the three individual TENGs tested. The justification for thicker electrodes is that it would collect more charge from the dissimilar material. The results determined thinnest

tape, TENG 3, produced the most power and had the highest power density of the three individual TENGs. Since TENG 3 had more interdigitated electrode fingers per bracket, which greatly increased the contact frequency and increased the power output. The size of the electrodes is not a factor that effects the power output but rather, the number of interdigitated electrode fingers. Less interdigitated fingers in TENG 1 caused the TENG to produces lower power. The lower contact frequency also means the time between peaks increases. The increased number ensures a more frequent contact between the PTFE tape and electrodes. This increases the frequency at which the electrons transfer, producing more charge per second, increasing the current output. Less interdigitated fingers in TENG 1 caused the TENG to produces lower power. The lower contact frequency also means the time between peaks increases.

Individually, nanogenerators do not produce enough power to have practical use, however, when connected, their power will multiply. TENG 4 and TENG 5 were to test if placing TENG in series or parallel would provide the most optimum performance. TENG 5 produced the most optimum output. This shows TENG in parallel is the most optimal orientation to produce optimal output. Placing the TENG in series increases the voltage but does not increase the amount of current it can produce. According to Kirchhoff's Law, $I_1 + I_2 = I_3$, which means the current from the first source will add to the second source and produce the final current. The TENG in parallel increases the amp-hour capacity which in turn will increase the charge generated from the TENG.

The TENG is designed to harvest ocean waves and determine if rotational motion produces a useable amount of energy. The purpose of the motor is to act as the external driving force for the inner rod for the TENG to produce power. The different speeds simulate the different frequencies for ocean waves. Even though 60 and 120 rpm can seem like a high frequency, when converted to Hertz, it is 1 and 2 Hz respectively. The motor speed for 240 and 360 rpm is equivalent to 4 and 6 Hz respectively.

V. CONCLUSION AND FUTURE WORK

A. CONCLUSION

This experiment is a continuation of the previous NPS design and tests the feasibility of using rotational motion in a TENG to generate electricity. It emulates previous NPS designs because it utilizes friction between copper and PTFE to generate electricity. The major difference is previous experiments utilize linear reciprocating motion. The TENG is consists of a rod spinning inside of a bracket vice a linear sliding mechanism to allow contact between the materials. A 3D printer constructed both components. The bracket contained two sets of interdigitated electrode fingers consisting of copper in varying sizes. The inner rod contained PTFE tape cut to the same width as the copper electrodes. The inner rod is connected to a DC motor and placed inside the bracket. After fastening the bracket to a rig, the DC motor spins at various speeds.

The main objective for the experiments is to determine if rotational motion for the TENG produces a higher power output than linear motion. The tests proved rotational TENGs produce more continuous power. The rotational TENG produced current that was higher than previous tests. At 2 Hz, the previous NPS TENG produced a maximum of 20 nA for current while at 120 rpm, equivalent to 2 Hz, produced an average of 50 nA. When combined in parallel, the TENG 5 produced an average current of 120 nA. When combined with other TENG, the TENG becomes much more effective. The motor for this experiment is the driving force for the inner rod that caused the TENG to produce power. Ideally, the improved design will use the wave motion to spin the inner rod and produce more power. The challenge lies with converting the linear motion from the ocean waves in to rotational motion from the TENG.

One other objective is to develop an TENG that is affordable and easy to reproduce. Copper tape is very affordable and easy to reproduce and remained adhered to the TENG bracket after several runs. The copper had several advantages that include manufacturing, accessibility, and replaceability. Copper tape is a common item and can be found in the gardening section of any hardware store. The only issue is to ensure the tape is pure copper,

which is remedied by placing a sample of the tape into the SEM. Cutting the copper into the appropriate shapes and sizes did not take very long after drafting the design on the Cricut application. Reproducibility facilitated replacing the damaged electrodes because the tape was easy to peel and reapply to the TENG. Cost is a big factor with the TENGs because individually, they do not produce ample power. Their power multiplies after connecting several in parallel. This keeping the cost low would allow energy companies to create a budget the TENG for mass production without overspending.

There were three different sizes for the experiment to test to determine which was most effective. While combining the two TENGs in series granted the highest power output, TENG 3 proved to have the highest power density. As determined through previous NPS experiments from ENS Sarah Reilly and LT Katherine Mann, the frequency of contact between the two materials was the determining factor for the output. TENG 3 has the most interdigitated electrode fingers attached to the outer bracket in comparison to the other two sizes of TENGs. The reduced width allowed for a shorter contact time between the two materials and increased contact frequency.

Power is directly proportional to the motor speed, therefore at higher speeds, the power output is much higher than lower speeds. The voltage and current increase linearly as the speed increases. TENGs are special because they can produce power at lower frequencies. The problem with the TENG is it produces such a low current, producing very low power. Connecting several TENGs in series remedies this issue as demonstrated in the results with the combination TENG. The TENGs in series showed promising results because the voltage made a significant increase upon connection.

The motor used to drive the inner rod in the TENG simulates an external force that results in producing electrical power. The external force may come from wind or ocean energy, etc. On the other hand, the TENG system may be considered for an existing rotational system such as a shaft which was already driven by an electric motor. In that case, one of the questions is how much additional electric power is required because of the TENG system and how much electric power is generated from the TENG system. If the latter is greater than the former, a net electric power would be generated from the system. The additional electric power should be converted to the mechanical power to overcome

the friction in the installed TENG system. Mechanical power for the rotational TENG is equal to the product of torque and angular velocity. Since frictional force is the major factor for torque, the TENG must overcome it to produce electrical power. For the TENG to be feasible, the electrical output must be greater than the power to overcome the frictional force. One way to reduce the power needed to overcome the frictional force is to reduce the coefficient of friction by experimenting with different surface finishes such as polishing the copper electrodes.

B. RECOMMENDATIONS

The major issue with experimentation is gathering the data for the current for the TENGs. The high current for a TENG is in the microamps but is typically in the nanoamps and can get as low as the picoamps. The Keithley 617 electrometer can read very low currents, however, it is outdated, and its cycle does not provide enough data points to make conclusions. The electrometer also does not have a simplified means to extract information. A newer version with a simpler method to export information. The other issue with this device is its frequency for its readings is very low and can potentially miss the readings. The other issue with this device is its sensitivity. Any subtle moves can distort the measurements for the device. This issue can be mitigated with a shielded probe or a higher quality probe.

The TENG is intended to be placed in water, therefore a waterproof material is more ideal. PLA is a durable material that is very easy to print. The issues with PLA are its rigidity and its water solubility. One concept for this TENG was to have a compressible material that would wrap around the inner rod. PLA is very rigid and will likely crack before it bends. One idea is to print TPU and line the bracket that would compress around the inner rod. The problem with TPU is it is a difficult material to work with in the printer that requires very specific settings. Training will give a better understanding of the material and proper settings to print this material. PLA is very water soluble, which means it will likely warp when exposed to humidity or water. This is not ideal for a generator designed to work in water. Possible materials to substitute are nylon and PETG. PETG is a commonly available material that has very similar properties as PLA.

For this experiment, one motor drove the single TENG and the TENG in series. Future experiments can utilize multiple motors, running at different speeds to simulate different wave heights and randomness. This could also aid in driving several TENG simultaneously. This will also give a better understanding on the number of TENG it takes to produce a substantial amount of power.

C. FUTURE RESEARCH

Rotational motion allows the TENG to operate in frequencies ranging from low to high. This provides a more consistent result for power output. The issue with collecting energy through rotational motion is it will gather energy from vertical and linear motion from ocean waves. Future work will involve converting linear motion into rotational motion to power the TENG. Attaching gears on the sides of the TENG will make the TENG spin faster by changing the gear ratios. This will increase the speed for the TENG and increase the contact frequency, therefore producing more power for the system. The goal for the TENG is to harvest ocean waves for the system. A waterproof case for the TENG is required for it to operate in the ocean but will provide a challenge when connecting multiple TENG in series.

This experiment was a proof of concept for TENG to test whether rotational motion is feasible. There are few designs for TENG that utilize rotation to generate power because ocean waves are linear motion. A future design for TENG is to convert the linear motion from the ocean waves into rotational motion. Another use for rotational TENG is to apply it to naval vessels and utilize the ocean drag to spin a turbine that would have the TENG produce power.

APPENDIX

The following graphs represent the current readings for each TENG at their respective sizes. Each graph displays the current information for each of the TENG at various speeds. The current data is from the Keithley 617 electrometer and the graphs display the current in nanoamps vs time. The maximum time is 20 seconds. The remaining graphs were exported from the Tektronix MSO4034 and display the voltage information for the each TENG at varying speeds of 360, 240, 120, and 60 rpms. Each graph is scaled to one sample per 200 milliseconds and each graph has 1000 samples. The graphs are voltage vs the number of samples, which displays information over 3 minutes and 40 seconds.

A. TENG 1 DATA

Figure 65 shows the current data for TENG 1. The current is very unstable at all speeds. This was the determining factor that prevented using it for further tests in TENG 4 and TENG 5.

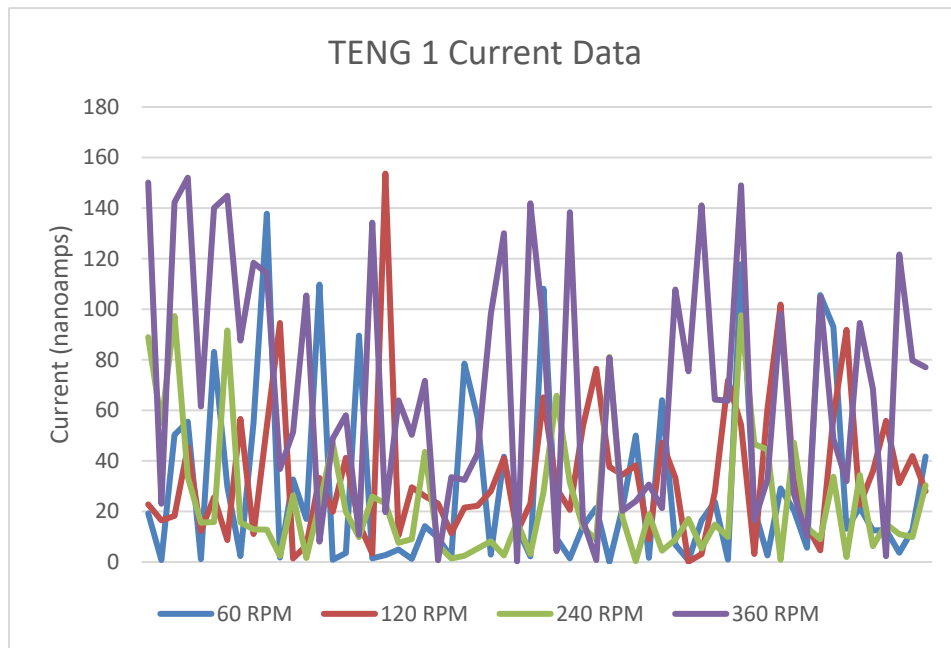


Figure 65. TENG 1 current readings for each speed.

Figures 66 to 69 show the voltage peaks for the TENG at various speeds. As the speed decreases the time between the peaks begins to increase. This is because the contact frequency decreases, gathering less charge.

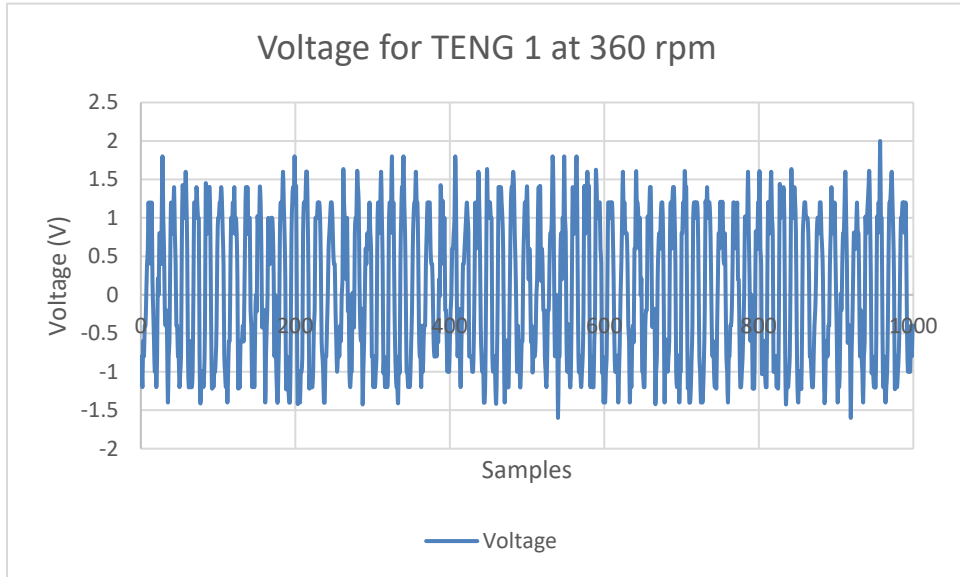


Figure 66. Voltage for TENG 1 at 360 rpm.

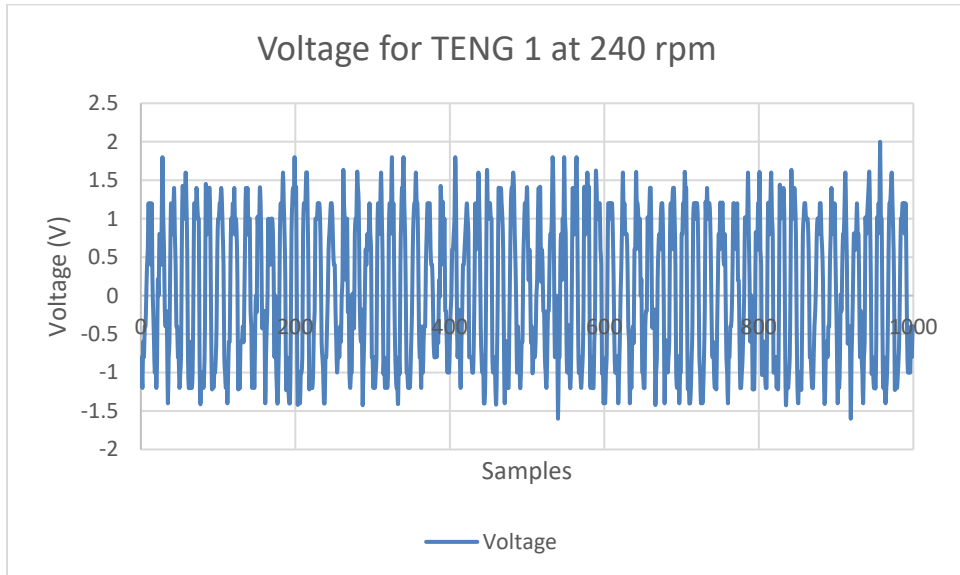


Figure 67. Voltage for TENG 1 at 240 rpm.

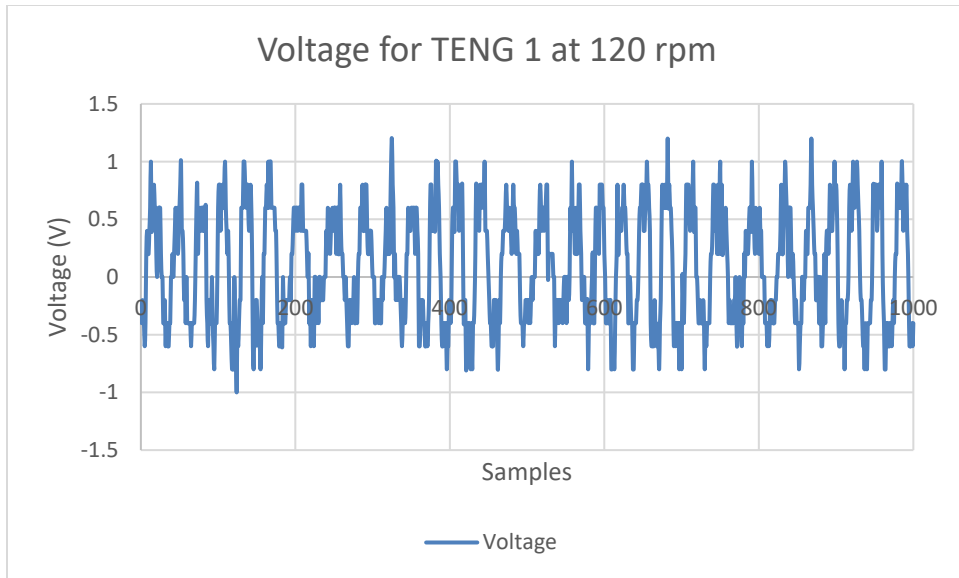


Figure 68. Voltage for TENG 1 at 120 rpm.

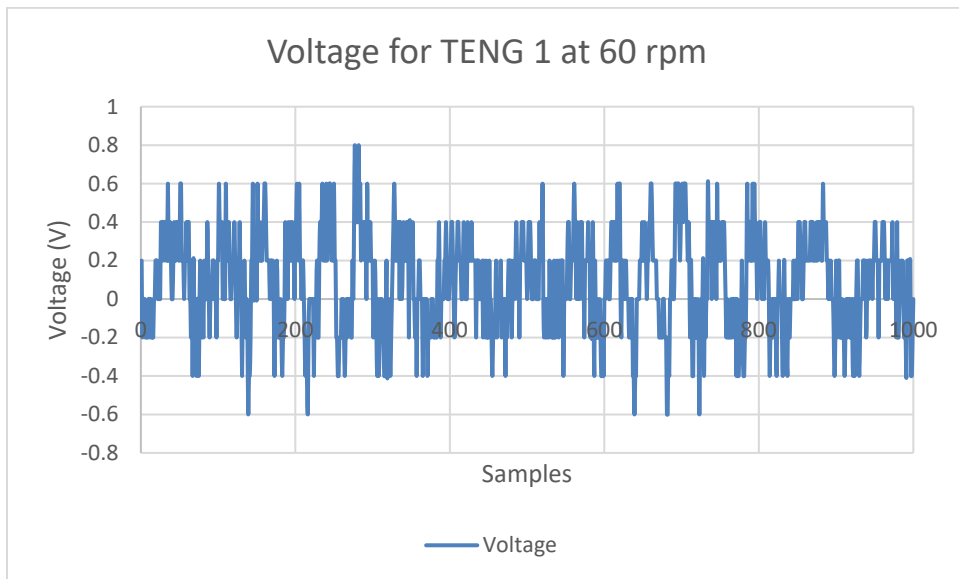


Figure 69. Voltage for TENG 1 at 60 rpm.

At very low speeds, 60 rpms, the time between peaks nearly quadruples.

B. TENG 2 DATA

Figure 70 shows the current data for TENG 2 at the set speeds. It is much more stable than TENG 1 at the higher speeds. The current becomes unstable once it reaches the

lower speeds. Its stability is the reason it is incorporated into TENG 4 and TENG 5 to test them in series and parallel.

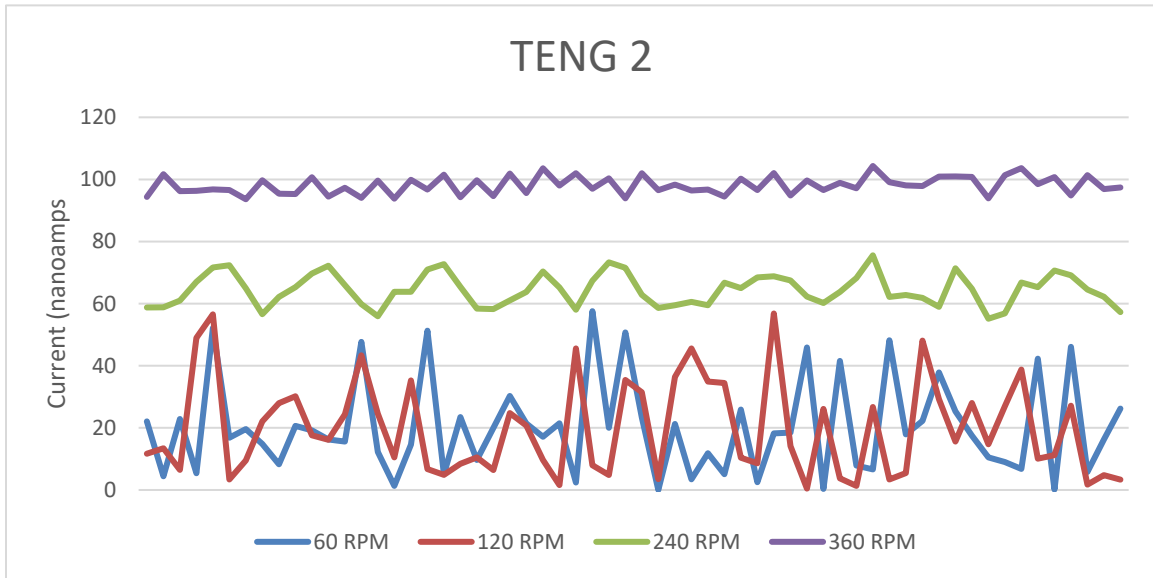


Figure 70. TENG 2 current readings for each speed.

Figures 71 to 74 display the voltage readings for TENG 2 at varying speeds.

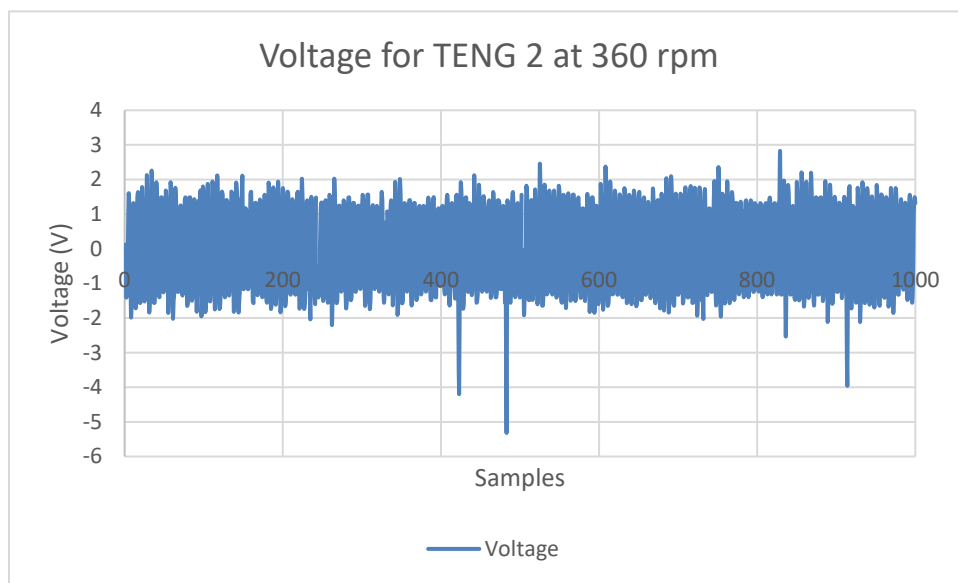


Figure 71. Voltage for TENG 2 at 360 rpm.

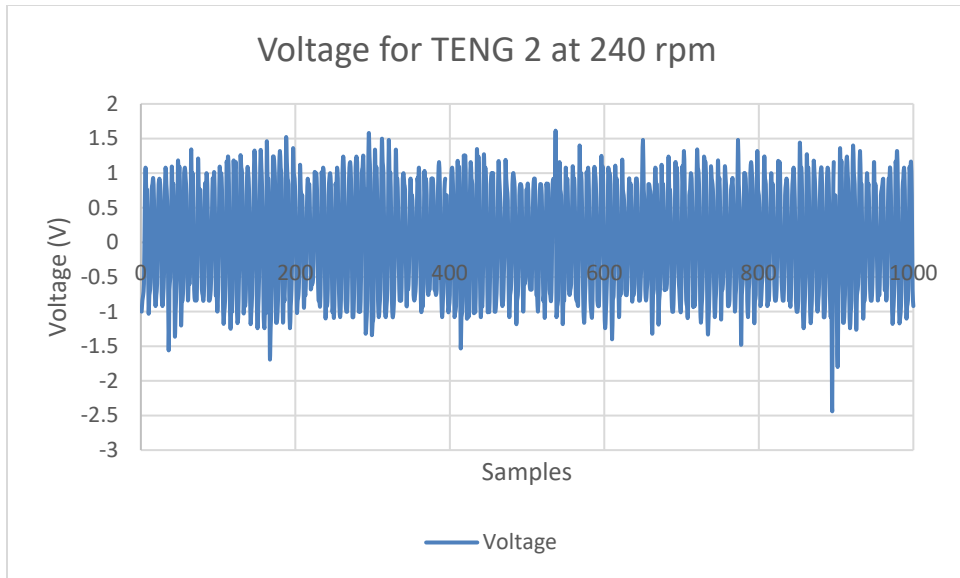


Figure 72. Voltage for TENG 2 at 240 rpm.

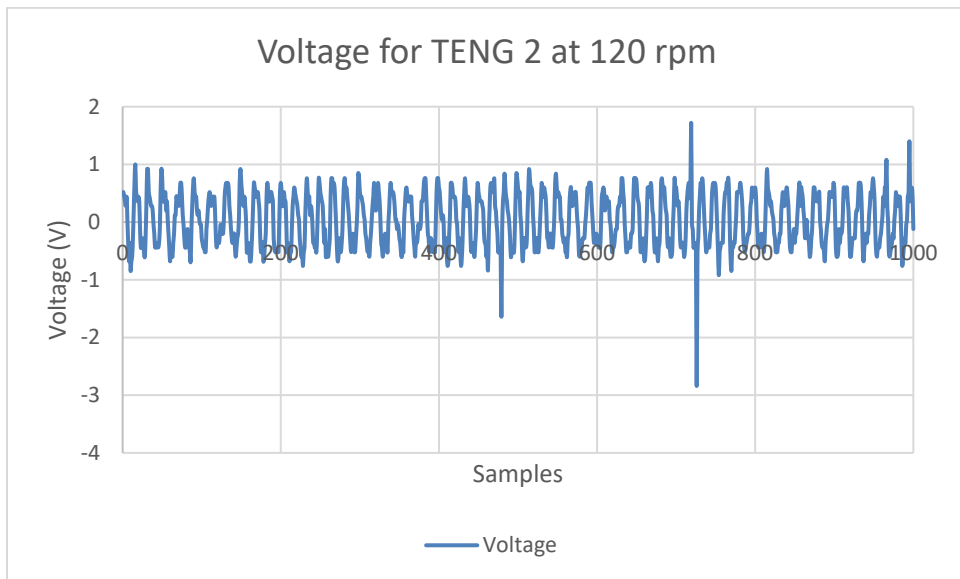


Figure 73. Voltage for TENG 2 at 120 rpm.

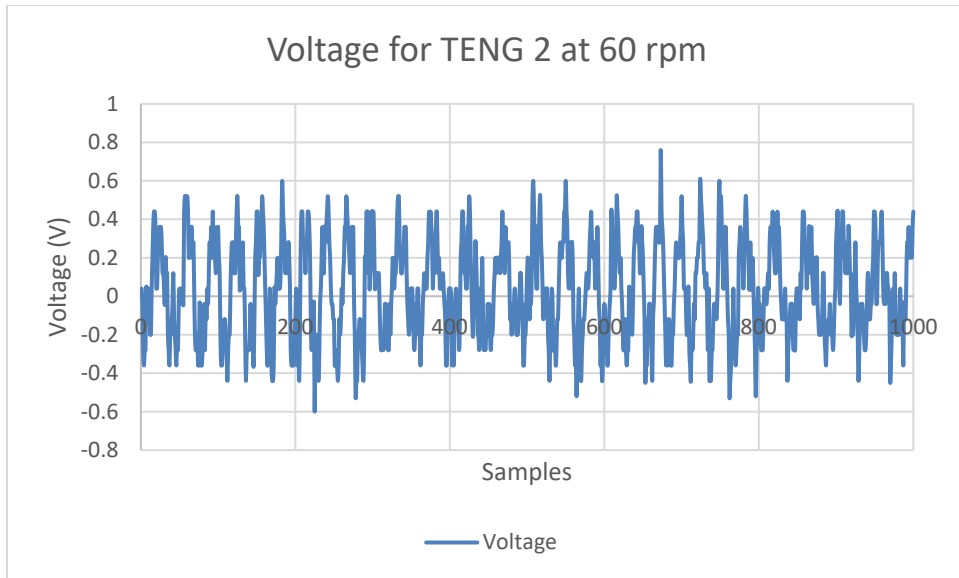


Figure 74. Voltage for TENG 2 at 60 rpm.

Like TENG 1, the time between peaks increases as the speed decreases as well as decreasing the voltage output.

C. TENG 3 DATA

Figure 75 displays the current data for TENG 3. Notice that the current is very stable up to at lower speeds. The current begins to show instability at 60 rpm. This size of TENG shows it is the most versatile TENG of the three designs, producing a stable power at very low speeds.

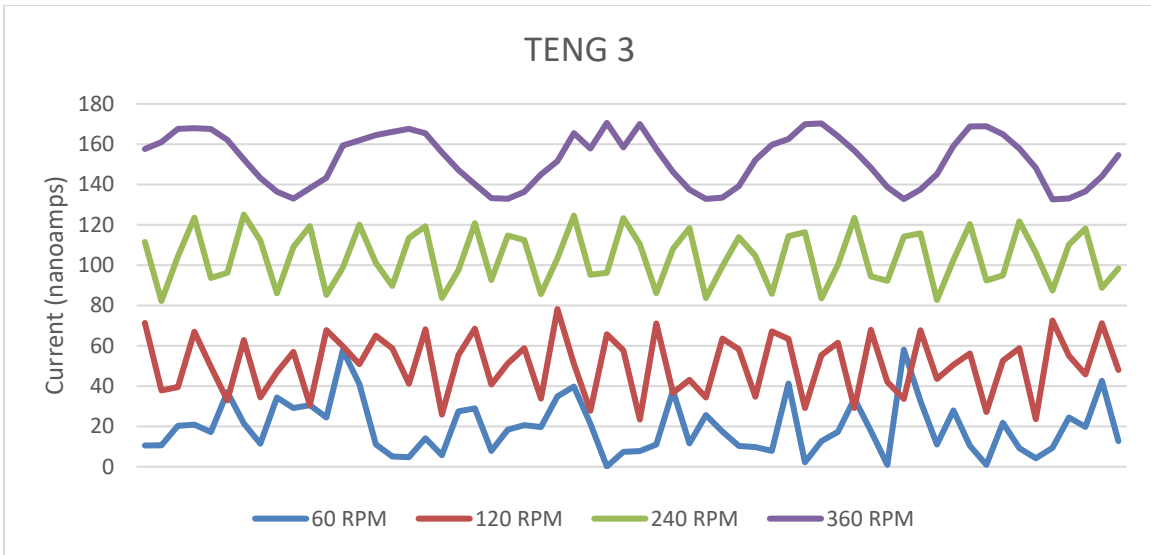


Figure 75. TENG 2 current readings for each speed.

Figures 76 to 79 display the voltage reading for TENG 3 at various speeds. The peak for the voltages is the highest of the individual TENG, however, the time between each peak is greater. This reduces the average time for this TENG. It has the highest maximum voltage of all the TENG.

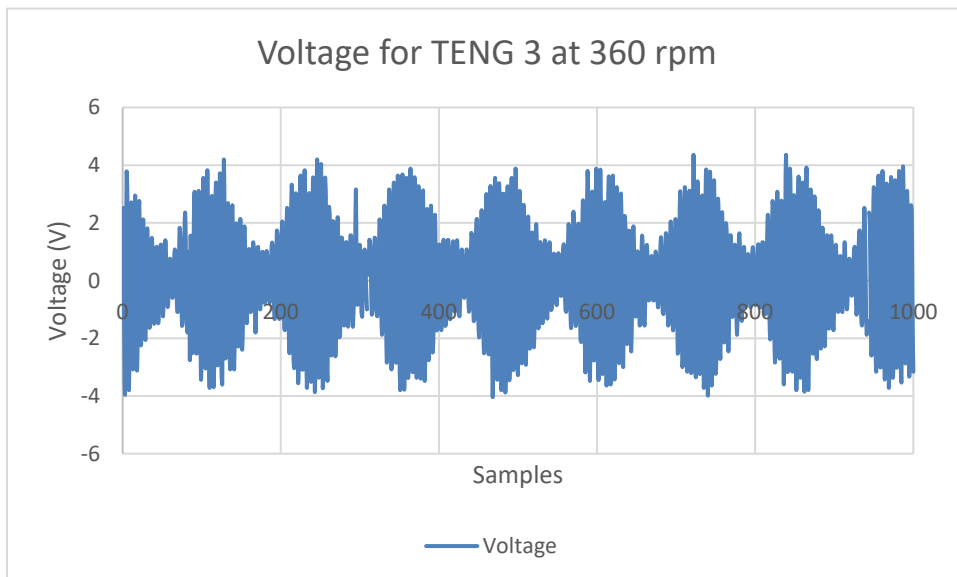


Figure 76. Voltage for TENG 3 at 360 rpm.

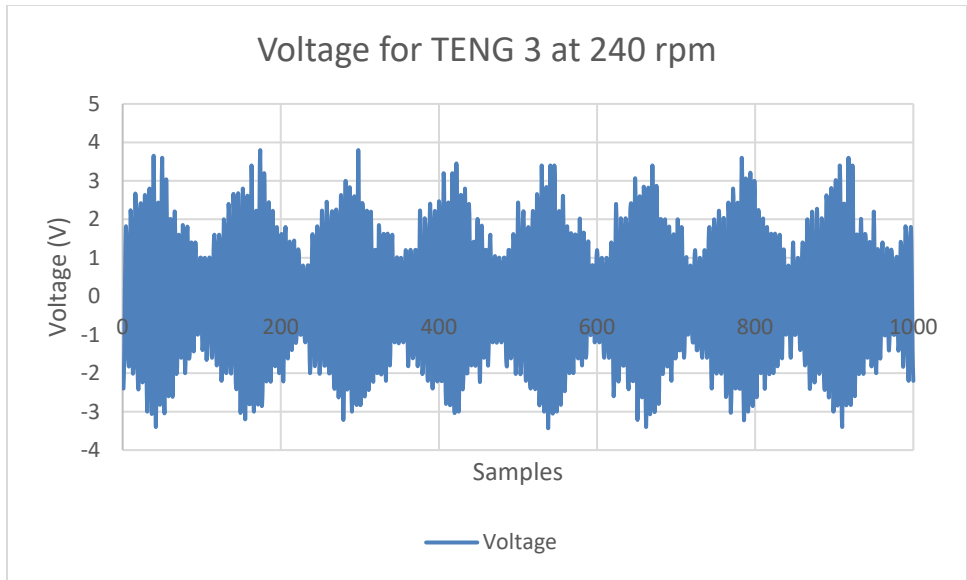


Figure 77. Voltage for TENG 3 at 240 rpm.

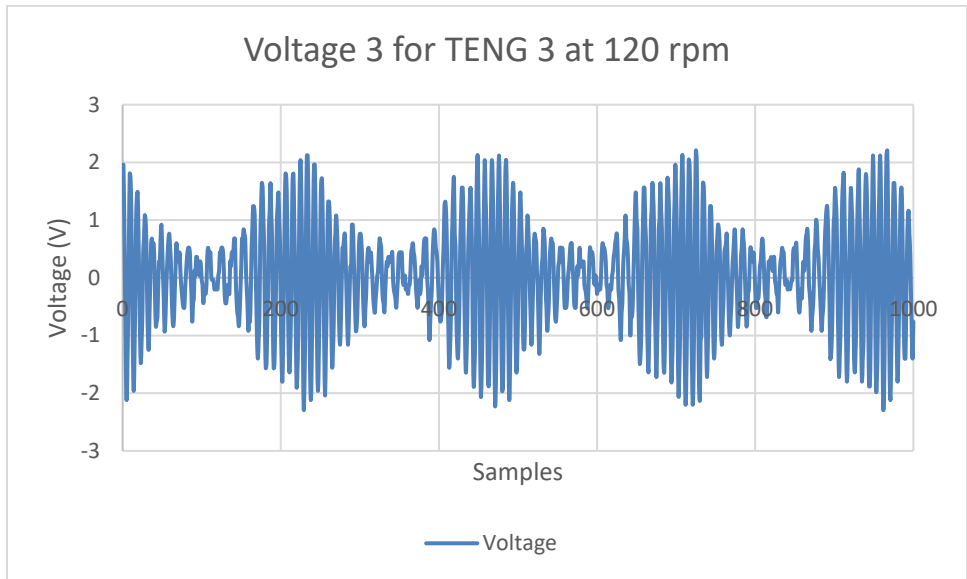


Figure 78. Voltage for TENG 3 at 120 rpm.

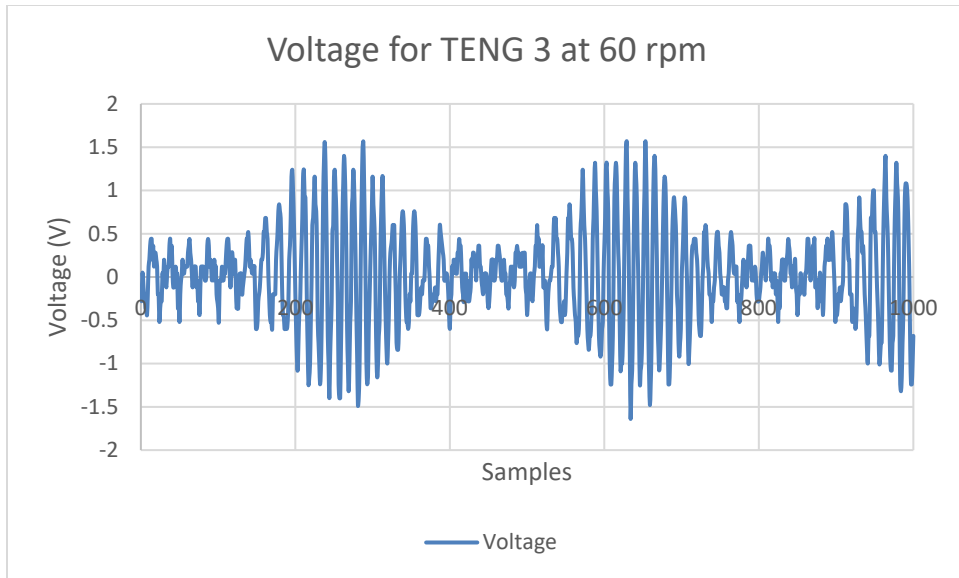


Figure 79. Voltage for TENG 3 at 60 rpm.

TENG 3 has the highest peaks of the individual TENG, however, at lower speeds, the time between peaks greatly affects average voltage output.

D. TENG 4 DATA

Figure 80 shows the current data for TENG 4, which is the TENG in series. TENG 4 is similar to the current data in TENG 3 that shows stability until it reaches 60 rpm. The current is slightly higher than TENG 3, which is an interesting result as the current should not increase when the power source is placed in series.

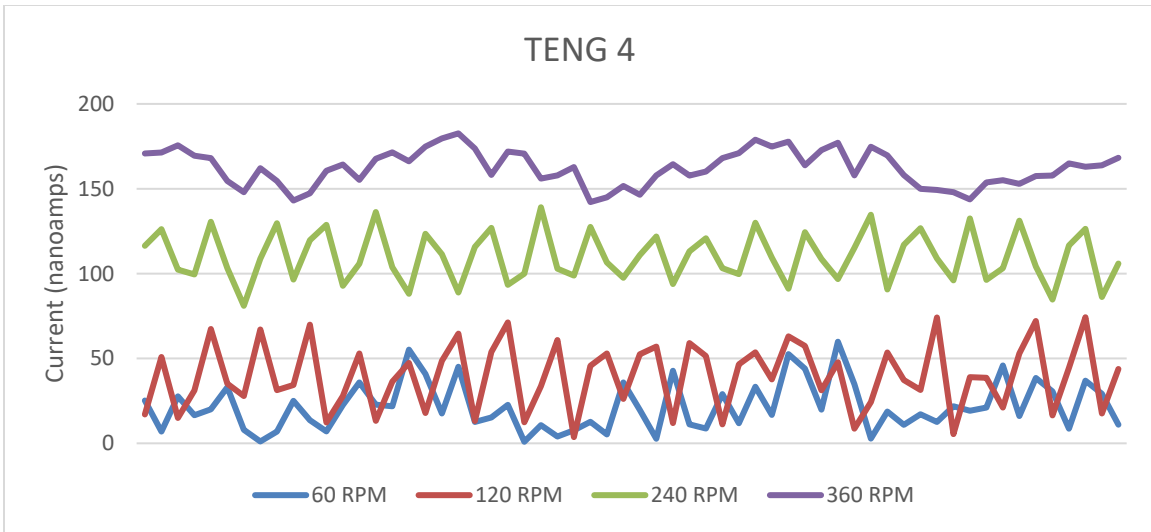


Figure 80. TENG 4 current reading for each speed.

Figures 81 to 84 show the voltage data for each run. The voltage increased compared to the individual TENG.

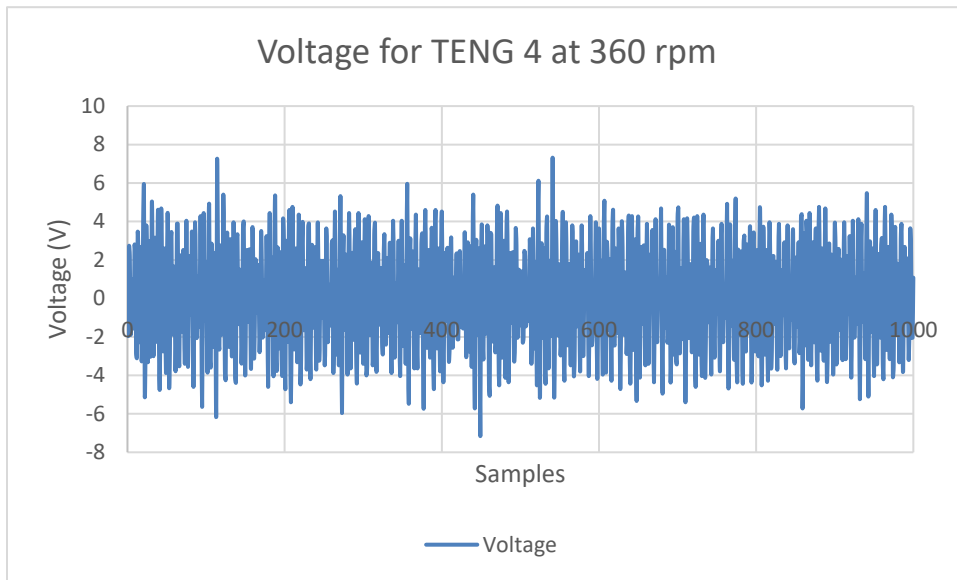


Figure 81. Voltage for TENG 4 at 360 rpm.

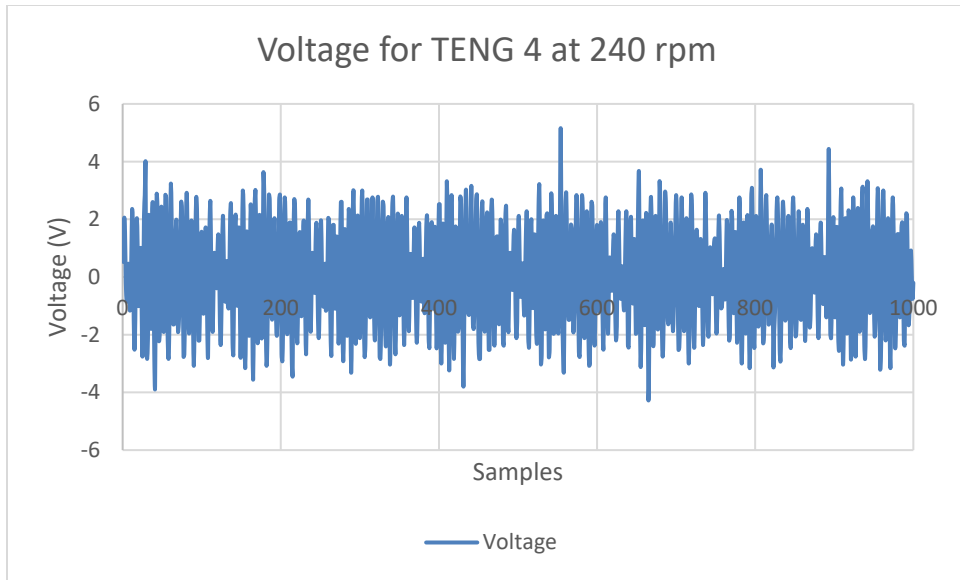


Figure 82. Voltage for TENG 4 at 240 rpm.

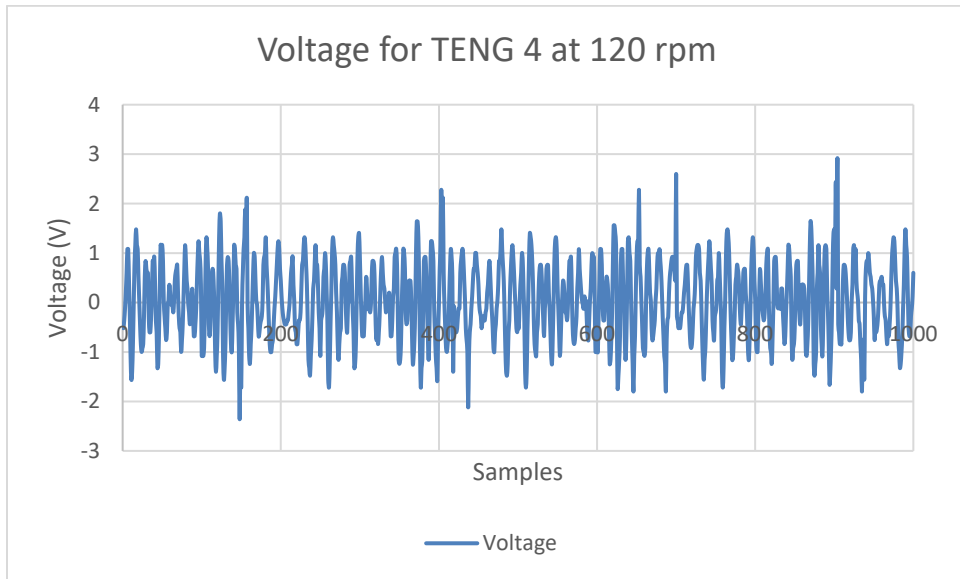


Figure 83. Voltage for TENG 4 at 120 rpm.

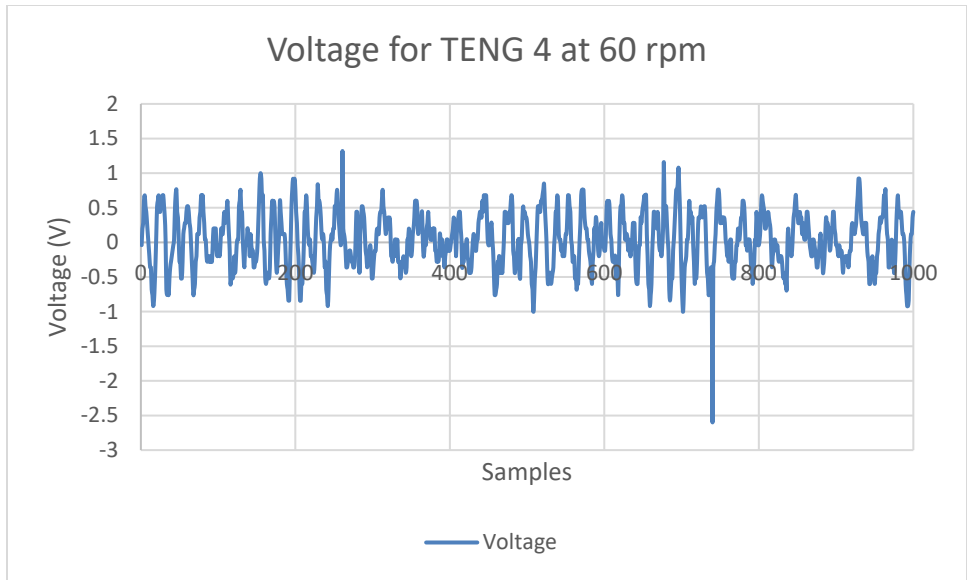


Figure 84. Voltage for TENG 4 at 60 rpm.

At lower speeds, TENG 4 produces a significant amount more voltage than the tests for individual TENGs.

E. TENG 5 DATA

Figure 85 shows the current data for TENG 5.

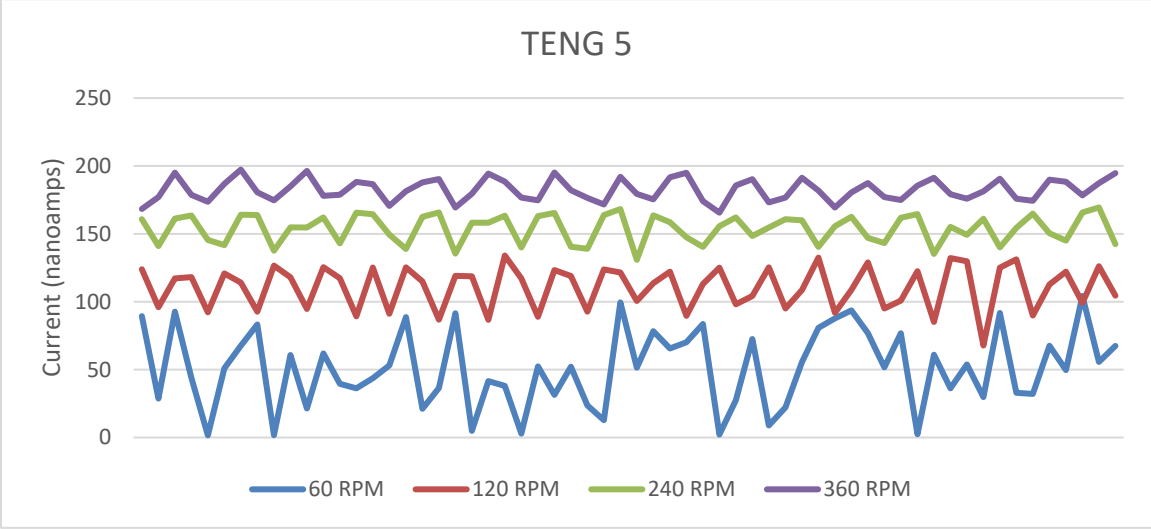


Figure 85. TENG 4 current reading for each speed.

The current for TENG in parallel is significantly higher and more stable than the other tests with TENG. At lower speeds, this TENG has a stable reading, which means it can produce a more stable power with low wave frequency.

Figures 86 to 89 display the voltage for TENG 5 at varying speeds. TENG 5 produced the highest voltage output for all the tests for TENG. This proves that having the TENG in parallel will produce optimal power.

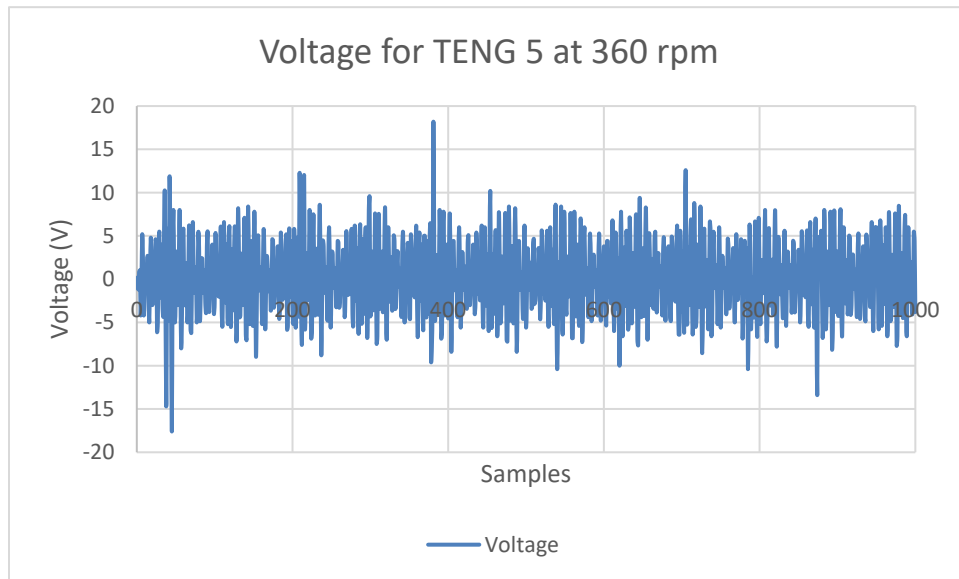


Figure 86. Voltage for TENG 5 at 360 rpm.

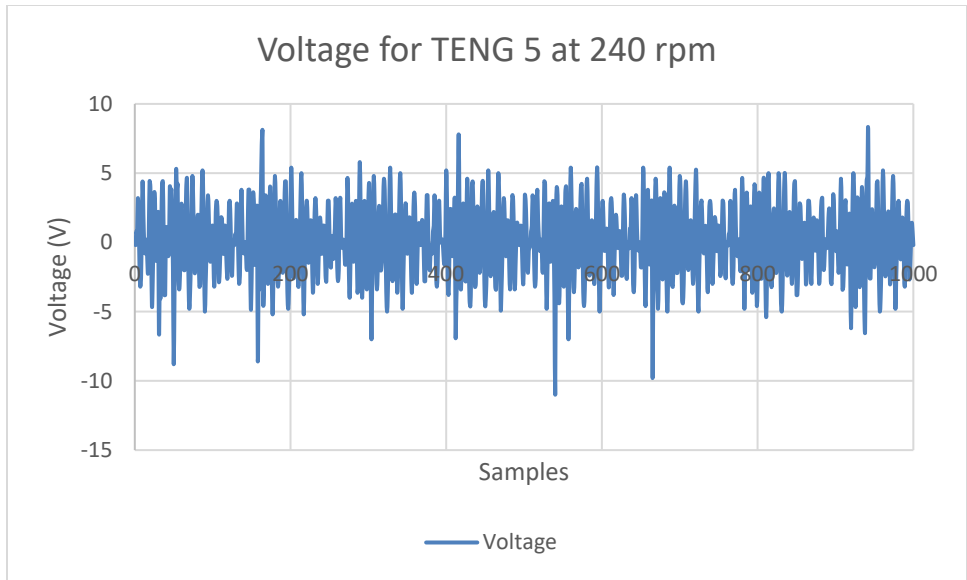


Figure 87. Voltage for TENG 5 at 240 rpm.

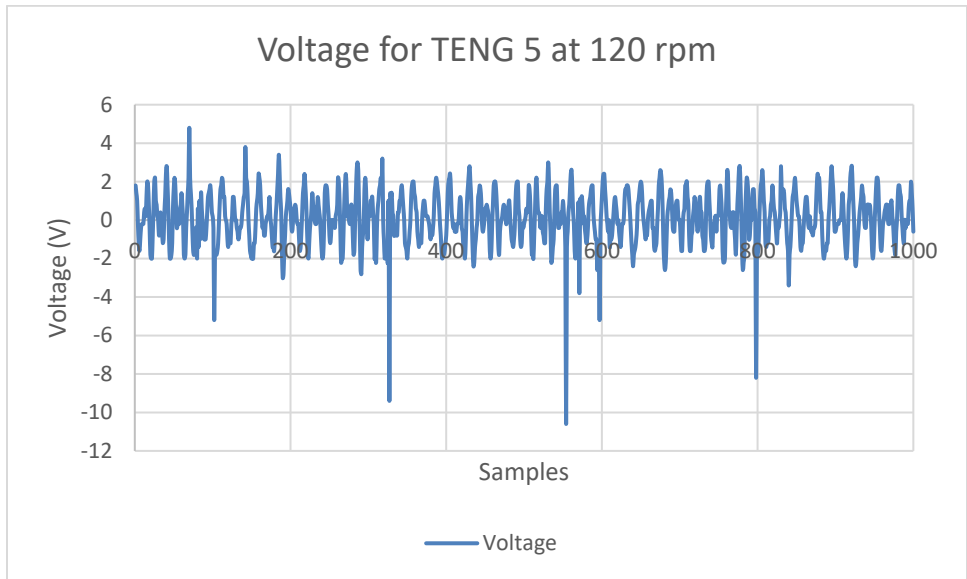


Figure 88. Voltage for TENG 5 at 120 rpm.

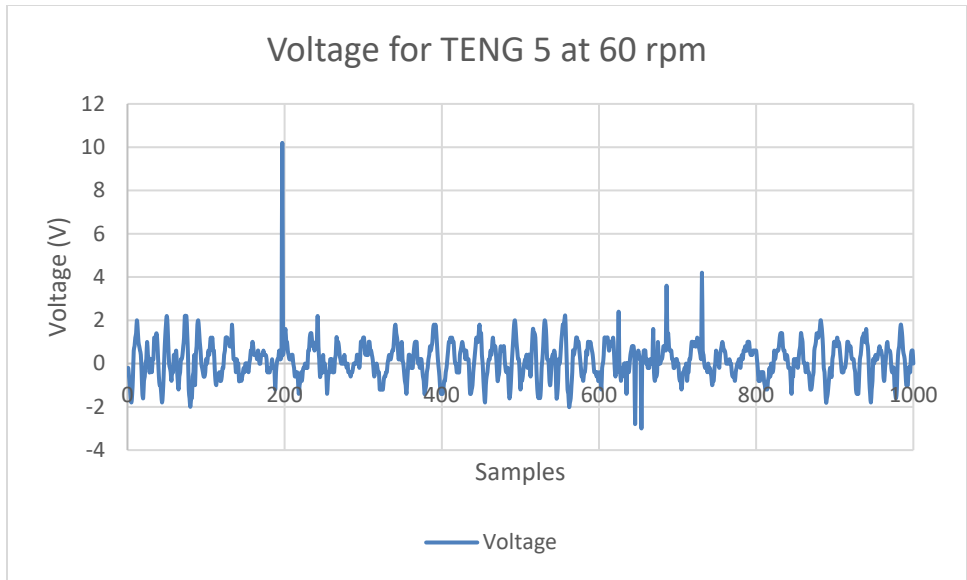


Figure 89. Voltage for TENG 5 at 60 rpm.

THIS PAGE INTENTIONALLY LEFT BLANK

LIST OF REFERENCES

- [1] “U.S. Energy Information Administration – EIA – Independent statistics and analysis.” *How much energy does a person use in a year? – FAQ – U.S. Energy Information Administration (EIA)*. [Online]. Available: <https://www.eia.gov/tools/faqs/faq.php?id=85&t=1>. Accessed March 10, 2019.
- [2] Z. L. Wang, “Triboelectric nanogenerators as new energy technology and self-powered sensors – Principles, problems and perspectives,” *Faraday Discuss.*, vol. 176, pp. 447–458, 2014.
- [3] Z. L. Wang, “On Maxwells displacement current for energy and sensors: the origin of nanogenerators,” *Materials Today*, vol. 20, no. 2, pp. 74–82, 2017.
- [4] J. Chen, J. Yang, Z. Li, X. Fan, Y. Zi, Q. Jing, H. Guo, Z. Wen, K. C. Pradel, S. Niu, and Z. L. Wang, “Networks of triboelectric nanogenerators for harvesting water wave energy: A potential approach toward blue energy,” *ACS Nano*, vol. 9, no. 3, pp. 3324–3331, 2015
- [5] Z. Wen, H. Guo, Y. Zi, M.-H. Yeh, X. Wang, J. Deng, J. Wang, S. Li, C. Hu, L. Zhu, and Z. L. Wang, “Harvesting broad frequency band blue energy by a triboelectric–electromagnetic hybrid nanogenerator,” *ACS Nano*, vol. 10, no. 7, pp. 6526–6534, Oct. 2016.
- [6] M.-L. Seol, J.-W. Han, D.-I. Moon, K. J. Yoon, C. S. Hwang, and M. Meyyappan, “All-printed triboelectric nanogenerator,” *Nano Energy*, vol. 44, pp. 82–88, 2018.
- [7] G. Zhu, P. Bai, J. Chen, and Z. L. Wang, “Power-generating shoe insole based on triboelectric nanogenerators for self-powered consumer electronics,” *Nano Energy*, vol. 2, no. 5, pp. 688–692, 2013.
- [8] Y. Mao, D. Geng, E. Liang, and X. Wang, “Single-electrode triboelectric nanogenerator for scavenging friction energy from rolling tires,” *Nano Energy*, vol. 15, pp. 227–234, 2015.
- [9] S. Reilly, “Triboelectric nanogenerator with ocean wave energy,” M.S. thesis, Dept. of Mechanical Engineering, NPS, Monterey, CA, USA, June 2019. [Online]. Available: <http://hdl.handle.net/10945/62717>
- [10] K. Mann, “Triboelectric nanogenerator for energy harvesting,” M.S. thesis, Dept. of Mechanical Engineering, NPS, Monterey, CA, USA, December 2019. [Online]. Available: <http://hdl.handle.net/10945/64018>

THIS PAGE INTENTIONALLY LEFT BLANK

INITIAL DISTRIBUTION LIST

1. Defense Technical Information Center
Ft. Belvoir, Virginia
2. Dudley Knox Library
Naval Postgraduate School
Monterey, California